Response of Ising systems to oscillating and pulsed fields: Hysteresis, ac, and pulse susceptibility

Muktish Acharyya* and Bikas K. Chakrabarti†
Saha Institute of Nuclear Physics, 1/AF Bidhannagar, Calcutta 700064, India
(Received 26 September 1994; revised manuscript received 20 March 1995)

We have studied, using Monte Carlo (MC) simulation for ferromagnetic Ising systems in one to four dimensions and solving numerically the mean-field (MF) equation of motion, the nature of the response magnetization $m(t)$ of an Ising system in the presence of a periodically varying external field $[h(t)=h_0\cos(\omega t)]$. From these studies, we determine the m-h loop or hysteresis loop area $A(=\oint m dh)$ and the dynamic order parameter $Q(=\oint m dt)$ and investigate their variations with the frequency (ω) and amplitude (h_0) of the applied external magnetic field and the temperature (T) of the system. The variations in A are fitted to a scaling form, assumed to be valid over a wide range of parameter (ω, h_0, T) values, and the best-fit exponents are obtained in all three dimensions $(D=2,3,4)$. The scaling function is Lorentzian in the MF case and is exponentially decaying, with an initial power law, for the MC cases. The dynamic phase boundary (in the h_0-T plane) is found to be frequency dependent and the transition (from $Q\neq 0$ for low T and h_0 to $Q=0$ for high T and h_0) across the boundary crosses over from a discontinuous to a continuous one at a tricritical point. These boundaries are determined in various cases. We find that the response can be generally expressed as $m(t)=P(\omega(t-\tau_{\rm eff}))$ where P denotes a periodic function with the same frequency ω of the perturbing field and $\tau_{\rm eff}(h_0,\omega,T)$ denotes the effective delay. We established that this effective delay $\tau_{\rm eff}$ of the response is the crucial term and it practically determines all the above observations for A, Q, etc. Investigating the nature of the in-phase (χ') and the out-of-phase (χ'') susceptibility, defined as $\chi'=(m_0/h_0)\cos(\phi)$ and $\chi''=(m_0/h_0)\sin(\phi)$; $\phi=\omega\tau_{\rm eff}$ [and m_0 is the amplitude of $m(t)$], we find that the loop area A is directly given by χ'' and also the temperature variation of χ'', at fixed ω and h_0, gives a prominent peak at the dynamic transition point. We have also studied the behavior of the response magnetization by the application of a short-duration (compared with the relaxation time) pulsed magnetic field. Here, we observed (both in the MC and MF cases) that the width ratio (of the half-width and the width of the response magnetization and of the pulsed field, respectively) and the susceptibility (the ratio of excess magnetization over its equilibrium value and the height of the pulsed field) both show sharp peaks at the order-disorder (ferromagnetic-paramagnetic) transition point. We have also studied similar response behavior of Ising systems in the presence of time-varying longitudinal and transverse fields, solving numerically the mean-field equation of motion. We have again studied here the nature of the dynamic phase transition and the behavior of the ac susceptibility (both longitudinal and transverse) across the dynamic phase boundary. For a short-duration pulse of the transverse field, the width ratio and the pulse susceptibility are again seen to diverge at the order-disorder transition point.

I. INTRODUCTION

When the external magnetic field on a ferromagnet is swept in time, say sinusoidally, the system cannot respond instantaneously, and the response gets delayed (in general with periodic but modified in form for its time variation). In particular, if the relaxation time of the (cooperatively interacting) thermodynamic system is comparable to the time period of the oscillating magnetic field, an interesting competition takes place. This leads[1] to the hysteresis loops, arising out of the delay in response to the driving field; a typical nonequilibrium phenomenon.

It is of considerable interest to study the nature of the response magnetization $m(t)$ of a magnetic system in the presence of such periodically varying external magnetic field $[h(t)=h_0\cos(\omega t)]$. It is observed that the thermodynamic response function is always periodic (although not necessarily sinusoidal, as the external field) with the same field frequency as that of the perturbing field, and gets delayed in general due to relaxation. The hysteresis loop is then identified as the Lissajous plot of the response function (m) versus the perturbing field (h). The delay in response gives rise to the nonvanishing width (loss) of the hysteresis loops. The equality in frequencies [of $h(t)$ and $m(t)$ and the delay in $m(t)$] gives rise to the quadratic equation for the Lissajous figures, giving the double valuedness and stability of the magnetization in the hysteresis loops.[1]

It is quite interesting to know how the hysteretic loss, or loop area $A(=\oint m dh$ over a complete cycle), varies with frequency ω and amplitude h_0 of the driving field and temperature T of the system. In the last few years there have been several theoretical studies[1–11] (and some experimental studies[12]) of the hysteretic response of various magnetic (model) systems. These theoretical investi-

gations can be classified into two classes.

(i) Theories without spatial fluctuations,[2-5] which reduce the dynamics of the system essentially to a single differential equation of the order parameter (the uniform magnetization in the mean-field approximation). In fact, as pointed out by Tome and Oliviera,[3] the numerical solution of the dynamical equation in the mean-field approximation for the response of a magnet in a periodically (e.g., sinusoidally) varying field indicates a novel dynamic phase transition: below a phase boundary $T_d(h_0,\omega)$, the dynamic order parameter $Q(=\oint m dt$; normalized over the time period of the field oscillation) or, the time-averaged magnetization (averaged over a complete cycle), acquires a nonzero value[3] [$Q=0$ for large T and h_0 values above $T_d(h_0,\omega)$ and $Q\neq 0$ for low h_0 and T; the boundary is in general frequency dependent]. This dynamic transition was later established for systems incorporating fluctuations.[1]

(ii) Theories considering spatial fluctuations may be further subdivided into two classes.

(a) For models with continuous excitations as in the n-vector model, the fluctuations can be tackled in the $n\rightarrow\infty$ limit. A numerical solution of the coupled differential equations by Rao, Krishnamurthy, and Pandit[6] suggests, in this limit, a power-law variation of the loop area (A) with frequency (ω) and the amplitude (h_0) of the externally applied sinusoidal magnetic field: $A\sim h_0^a\omega^b$ where $a=\frac{2}{3}$ and $b=\frac{1}{3}$ in the low ω (and $T<T_c$, the critical temperature for $h_0=0$) limit in two dimensions. As pointed out by Dhar and Thomas,[7] the corrected solution, with the allowance for (nonvanishing) transverse magnetization in the n-vector model in the $n\rightarrow\infty$ limit, suggests $a=b=\frac{1}{2}$, with logarithmic correction, for loop area variation.

(b) Other studies are for models with discrete excitations as in Ising models[1,8-10] in two to four dimensions using Monte Carlo simulations. These simulation results again confirmed a power-law fit for A, with $a\cong 0.46$ and $b\cong 0.36$ in dimension $D=2$[8,9] in Ising systems for very low ω and T limit. Lo and Pelcovits[8] also studied the dynamic transition. However, they could not determine the phase boundary $T_d(h_0,\omega)$ precisely. Acharyya and Chakrabarti[1] studied the scaling behavior for the variation of A with ω, h_0, and T over a wide range of variations and found

$$A\sim h_0^a T^{-\beta} g(\omega/h_0^\gamma T^\delta)\ , \tag{1}$$

with the scaling function

$$g(x)\sim x^\epsilon e^{-x^2/\sigma} \tag{1a}$$

in the Monte Carlo case, and

$$g(x)\sim x/(1+cx^2) \tag{1b}$$

or Lorentzian in the mean-field case. The best-fit values for the exponents were found in dimensions $D=2$, 3, and 4 in the mean-field case. This scaling form reduces to a power law in the $\omega\rightarrow 0$ limit, giving

$$A\sim h_0^a\omega^b T^{-c}\ , \tag{1c}$$

with $a=\alpha-\epsilon\gamma$, $b=\epsilon$, and $c=b+\epsilon\delta$. Putting the values of the above exponents α, β, γ, δ, and ϵ, one gets $a\cong 0.70$, 0.67, and 0.32 and $b\cong 0.36$, 0.45, and 0.50 in $D=2$, 3, and 4, respectively. The values of a and b in $D=2$ are comparable with previous Monte Carlo[8] and cell dynamical estimates.[9] These studies also indicated that the variation of A with T is continuous without any signature of any singularity in $A(T)$ at any effective $T_c(>0)$. The existence of the "paramagnetic" loops was also confirmed by extrapolating finite-size studies and from studies on hysteresis in a one-dimensional chain.[1] The dynamic order parameter Q (or the time average magnetization, averaged over a complete cycle) acquires a nonzero value below a critical $T_d(h_0,\omega)$ line in the phase diagram, and extensive studies[1,11] for the dynamic phase transition were also made and the phase diagram $T_d(h_0)$ in the h_0-T plane had been obtained (for different ω) in $D=1$ to 4. The vanishing of the dynamic order parameter Q across the phase boundary becomes discontinuous (cf. Ref. 3) below a tricritial point $T_d^{\rm TCP}(h_0,\omega)$. These phase diagrams have been studied and the tricritical points have been located[1,11] in the Monte Carlo studies for one- to four-dimensional Ising systems and for the mean-field dynamics. As mentioned before, the response $m(t)$ is always periodic with the same period as that of the external field $h(t)$ [although $m(t)$ is not necessarily sinusoidal, except in the limit $h_0\rightarrow 0$ and $T\gg 1$]. The response, however, generally gets delayed compared to $h(t)$. We can thus express $m(t)$ as $P(\omega(t-\tau_{\rm eff}))$, where P induces the same periodicity (ω) as that of $h(t)$ and $\tau_{\rm eff}$ is the effective delay due to relaxation (determined in general by T, h_0, ω, etc.). Solving $m(t)$ for $h(t)$, one gets the quadratic equation (because of the same periodicity in m and h) for the Lissajous plots or the hysteresis loops.[1] Instead of solving for the hysteresis loops (Lissajous plots), we also studied[13] here the (linear) ac susceptibility $\chi=\chi'-i\chi''$, $\chi'=(m_0/h_0)\cos(\omega\tau_{\rm eff})$, and $\chi''(m_0/h_0)\sin(\omega\tau_{\rm eff})$, where m_0 is the amplitude of $m(t)$. We studied the variations of this ac susceptibility of an Ising system, using a numerical solution of the mean-field equation of motion for the dynamics and using the Monte Carlo dynamics for two- and three-dimensional systems. The properties of $\chi'$and χ'', in particular, their temperature and frequency variations, are obtained. These behaviors are also compared with those for conducting magnets.[14-16] It is found that χ' has a dip and χ'' has a sharp peak at the temperature $T_d(h_0,\omega)$ at which the dynamic phase transition occurs [$Q\neq 0$ for $T<T_d(h_0,\omega)$ and $Q=0$ above]. This indicates that the dynamic transition is a true thermodynamic phase transition. χ' has another smeared peak at a higher temperature. We thus found indications[13] of a new method to detect the dynamic phase transition[1,3] in such systems, from the study of temperature variations of χ'' (and χ') for fixed h_0 and ω. We report here some additional results for the ac susceptibility and its behavior near the dynamic transition.

We also report here the results of the response of an Ising system due to a pulsed magnetic field. We have studied the behavior of the response (magnetization) due to a pulsed field of very short duration (compared with the re-

laxation time), using Monte Carlo simulation and solving the mean-field equation. The form of the pulsed field is $h(t)=h_p$ for a short duration δt and $h(t)=0$, elsewhere. The pulse has been applied after bringing the system to its (thermodynamic) equilibrium state at any temperature. The response magnetization $m(t)$ also shows a sudden rise from its equilibrium value, which we characterize by its height m_p and half-width Δt. The width ratio $R \equiv \Delta t/\delta t$ and the pulse susceptibility $\chi^p \equiv m_p/h_p$ are studied. Both these quantities show sharp peaks at the order-disorder transition point. The usefulness of the studies of such (pulse) susceptibilities is indicated.

To see the quantum effects on phase transition behavior, the simple and widely studied Hamiltonian has been the Ising systems in transverse field.[17,18] Here, the tunability of the quantum fluctuation (through the manipulation of the transverse field or tunneling term) and its separation from the cooperative term give added advantage (for analytic study). The effect of such tunneling terms on finite temperature hysteresis in Ising systems has recently been studied by Acharyya, Chakrabarti, and Stinchcombe (ACS).[10] These studies have been extended here for oscillating and pulsed transverse field cases.

ACS studied,[10] by solving the dynamical mean-field equation for the components of the magnetization, the response of an Ising system in the presence of a (sinusoidally) oscillating transverse field. The hysteric loop area ($A_x = \oint m^x d\Gamma$, m^x denoting the transverse magnetization and Γ the transverse field) has been observed to fit to a scaling relation $A_x \sim \Gamma_0^{\alpha'} T^{-\beta'} g(\omega/\Gamma_0^{\gamma'} T^{\delta'})$, where α', β', γ', δ' are some exponents, T is the temperature of the system, and ω and Γ_0 are the frequency and amplitude of the transverse field, respectively. The scaling function $g(x)$ has been observed to be Lorentzian, having the form $x/(1+cx^2)$. The scaling exponents were estimated exactly by solving analytically the dynamical mean-field equation in some (linearized) limits. They also obtained the phase boundary (in the Γ_0-T plane) for the dynamic phase transition [where the order parameter is $Q_z = \oint m^z(t)dt$], across which Q_z changes from nonzero to zero values. An analytic estimate of the phase boundary has also been obtained [$T=\tilde{\Gamma}_0/\sinh(\tilde{\Gamma}_0)$, $\tilde{\Gamma}_0=(\pi/2)\Gamma_0$], which agrees well with that obtained numerically.

From the response of an Ising system in the presence of an oscillating longitudinal field and a static transverse field, we have also studied the dynamic transition boundary in the temperature T and the transverse field Γ plane. Here again, the ac susceptibility components show sharp peaks (or dips) at the dynamic transition point. The response magnetization of the transverse Ising system has also been studied for a short-duration pulse (of width δt and height $\delta\Gamma$, over its steady value Γ) of the transverse field. Induced response (due to pulsed transverse field) is seen to have finite width and height. The width ratio (of the half-width of the response with that of the pulse) and the pulse susceptibility (the ratio of the height of the induced response with that of the pulse) diverge at the order-disorder transition point. This study again indicates that the variation of this "pulse-width ratio" or the "pulse susceptibility" are very useful dynamical probes to determine the "static" phase diagram. These results are reported here.

We organize the paper as follows. In Sec. II, we discuss the results for the response of the classical Ising system, and in Sec. III the response of the quantum Ising system. In Sec. II A we present the Ising Hamiltonian and discuss the Monte Carlo technique employed and the mean-field dynamical equation of motion used. In Sec. II B, we give the results for the delayed response magnetization and compare that with the external field. In Sec. II C, we give the results for loop area variation and discuss the scaling fits. We give the results for dynamic transition in Sec. II D. In Sec. II E, the results for the study of the ac susceptibility in such systems and its variation across the dynamic phase boundary are discussed. In the next section (Sec. II F), we give the results of the response due to a pulsed field of very short duration.

In Sec. III, we extend the previous study[10] of hysteresis in the transverse Ising system by investigating the nature of response magnetization of an Ising system in the presence of a static transverse field and an oscillating longitudinal field, as well as for an Ising system in the presence of a short-duration (compared to the relaxation time) pulse of the transverse field. These studies have been made here using the mean-field (MF) equation of motion for the transverse and longitudinal magnetizations. The model Hamiltonian considered here and the MF dynamical equations are discussed in Sec. III A. The numerical results of the dynamic phase transition and the ac susceptibility variation with respect to temperature and transverse field are discussed in Secs. III B and III C, respectively. The results for the response magnetization due to an additional pulse in the tunneling field Γ, over a steady transverse field, are given in Sec. III D. Concluding remarks are made in Sec. IV.

II. RESPONSE OF THE ISING SYSTEM TO TIME-VARYING LONGITUDINAL FIELD

A. Monte Carlo simulation and mean-field dynamics

For Monte Carlo (MC) study we consider an Ising system with nearest-neighbor ferromagnetic interaction in the presence of a sinusoidally varying external longitudinal magnetic field. The Hamiltonian is taken as

$$H = -J \sum_{\langle i,j \rangle} \sigma_i^z \sigma_j^z - h(t) \sum_i \sigma_i^z , \tag{2}$$

where J (>0) is the nearest-neighbor ferromagnetic interaction strength, and $h(t)$ is the sinusoidally varying external magnetic field $h(t)=h_0 \cos(\omega t)$; ω is the frequency of the ac magnetic field. The spin variables σ^z can take only two (± 1) values. In our study, the scale of energy has been set by choosing $J=1$. We consider periodic boundary conditions for lattices of sites L, where $L=100$, 20, and 10 in $D=2$, 3, and 4, respectively (some of the results have been checked for much bigger sizes, e.g., for $L=1000$ and 100 in $D=2$ and 3, respectively). We used the standard Metropolis Monte Carlo algorithm (Glauber dynamics)[11] for simulating the Ising system.

We update the spin variables σ^z by stepping sequentially through the lattice. In our study, first we kept the temperature (T) and the field amplitude (h_0) fixed, and varied the frequency (ω) of the applied magnetic field. Here the unit time interval t is defined such that $t \times 12 \times 10^5$ equals unity. This choice, although arbitrary, has been made to ensure that for highest frequency (in our chosen range), the number of steps required to complete a cycle would be at least of the order of 10 [the minimum number of MC steps is of the order of 10 at high frequencies $\omega \sim O(10^5)$]. This Monte Carlo time (in units of single iteration over the entire sample) is not directly related to the real time. Various cluster algorithms could be used for faster updates. However, we believe the scaling properties (singularities in time or frequency variation) would remain unchanged for any such algorithms. The range of the field amplitudes is also suitably chosen: For low enough field amplitude, lower than coercive field, one would not get the conventional (symmetric) shape of the hysteresis loop. On the other hand, for very high field the cooperative effect would be suppressed and the magnetization saturates. The typical response function and the shapes of the loops for different parameter values h_0, ω, and T in $D=3$ are shown in Fig. 1(a). Most of the data on loop area, used in the later analysis, are obtained from averages over about 10 to 30 random number seeds.

For comparison, we also study the results of mean-field (MF) equations of motion. The equation for the dynamics of the magnetization (m) of a magnet in the presence of a sinusoidally time-varying magnetic field [$h(t)=h_0\cos(\omega t)$] may be written in the mean-field approximation as [1,3]

$$\tau\frac{dm}{dt} = -m + \tanh\left[\frac{m + h_0\cos(\omega t)}{T}\right] . \tag{3}$$

Here m represents the magnetization, h_0 and ω represent

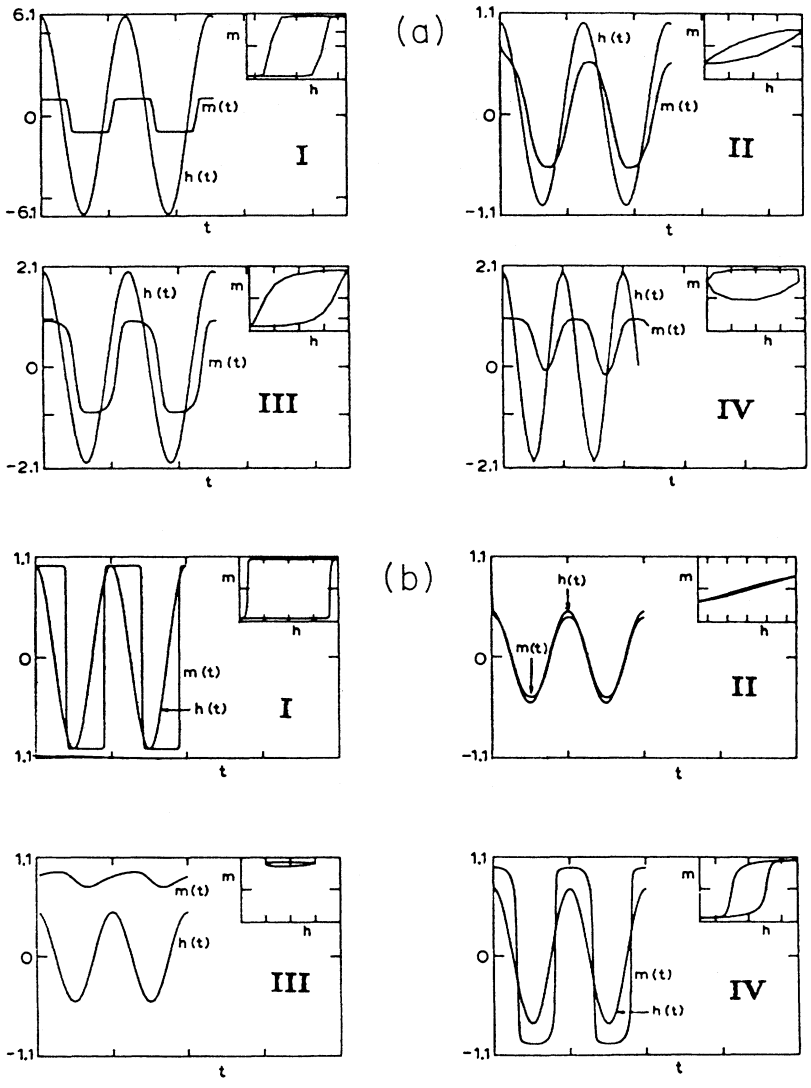

FIG. 1. Some typical time variations of response (magnetization) function with the (perturbing) field variation. The inset shows the corresponding Lissajous plots (hysteresis loops). (a) In the Monte Carlo study for the $D=3$ Ising case. I: $\omega=0.208$, $h_0=6.0$, and $T=2.0$; II: $\omega=0.208$, $h_0=1.0$, and $T=6.0$; III: $\omega=0.208$, $h_0=2.0$, and $T=4.0$; and IV: $\omega=0.524$, $h_0=2.0$, and $T=2.5$. (b) In the mean-field case. I: $\omega=0.006$, $h_0=1.0$, and $T=0.1$; II: $\omega=0.006$, $h_0=0.5$, and $T=2.0$; III: $\omega=0.314$, $h_0=0.5$, and $T=0.5$; and IV: $\omega=0.006$, $h_0=0.75$, and $T=0.75$.

the amplitude and the frequency, respectively, of the sinusoidally varying magnetic field, and T is the temperature of the system (the Boltzmann constant and the spin-spin interaction strength are taken to be unity). The τ here represents the microscopic (single spin-flip) relaxation time. We have solved the equation numerically both by discreatizing, i.e., using the map

$$m(t+\tau)=\tanh\left[\frac{m(t)+h_0\cos(\omega t)}{T}\right], \tag{3a}$$

and by using the fourth-order Runge-Kutta method (in single precision, taking the time differential equal to 10^{-6}) to get $m(t)$ from Eq. (3). Both give qualitatively the same results; the results obtained using Runge-Kutta are more accurate and we use those results. Plotting $m(t)$ as a function of $h(t)$ we got the m-h loop. Some of the typical response functions and the shapes of the loops are shown in Fig. 1(b).

B. Delayed response

1. Monte Carlo results

Here our main interest is in the study of the response function for periodic perturbation in such magnetic systems. We have shown in Fig. 1(a) some typical MC results for $d=3$ response functions (magnetization); the corresponding Lissajous figures (the hysteresis loops) are also shown. It may be noted from these figures (for the response magnetization behavior) that the response function (although delayed) is again a periodic function with the same frequency (ω) as the field. This is because of the invariance of the Glauber dynamics (see Ref. 11) to the replacement of the time t by $t+2\pi/\omega$, as the local field is a linear function of local spin moments and does not contain any time integral (noninvariant) operators. As mentioned earlier, this equality of the period of both the perturbation and the response is responsible for the quadratic nature of the Lissajous figures (see the Appendix) and the double valuedness (and stability) of the magnetization in the m-h or hysteresis loops. In fact, if the frequencies would be slightly different, the Lissajous figures would be unstable and would continuously change shape (see Appendix) with a periodicity dependent on the frequency mismatch. It may further be noted (from the response behavior shown in Fig. 1) that as the temperature of the system increases, the effective time lag (τ_{eff}) goes to zero and the hysteresis (or m-h) loop (width) shrinks and the loop area (A) tends to vanish (see the discussions in the next section). In fact, τ_{eff} is also a function of the amplitude h_0 (until saturation) and frequency ω of the perturbing field. The ω and T dependence of τ_{eff} are extracted from these MC results and will be discussed in Sec. II E.

2. Mean-field results

The nature of the response in this mean-field limit has been studied already by Tome and Oliviera.[3] In Fig. 1(b), we just give some typical response functions and the corresponding Lissajous plots (in the insets). Here again, the response is periodic with the same frequency as that of the ac magnetic field. This is because the equation of motion (3) is invariant under a replacement of t by $t+2\pi/\omega$. The effective delay (in time) τ_{eff} has also been extracted from these numerical results, and its variation with respect to temperature and also with the frequency ω of the external field will be discussed in Sec. II E.

3. General form of response magnetization

Generally, one can write the solution for the response function (magnetization) as

$$m(t)\sim P(\omega(t-\tau_{\text{eff}})), \tag{4}$$

where P is a function such that $m(t)$ is also periodic [having amplitude $m_0(T,h_0,\omega)$] with the same frequency ω of the perturbing field h. The delay in the response by the effective time lag τ_{eff}, compared to the perturbing field $h(t)$, will be studied in Sec. II E.

C. Loop area

Scaling

We observed that for a particular temperature and field amplitude, initially the area increases with frequency and reaches a peak, dependent on h_0 and T. After that, it decreases as frequency increases further. The whole curve rises up and the peak shifts towards the low-frequency side as the temperature is lowered (for fixed field amplitude). Similarly, at any fixed temperature, the whole curve rises up and the peak shifts towards the high-frequency side as the field amplitude is raised. This is a common feature for all dimensions [see insets of Figs. 2(a)–2(d)]. We tried to fit all these results for $A(h_0,\omega,T)$ to the scaling form Eq. (1) with the scaling function $g(x)$ given by Eq. (1a) [see Figs. 2(a)–2(d)]. The best-fit values for the exponents α, β, γ, δ, and ϵ in different dimensions are given in Table I. Note that these exponent values are the best-fit values (over a wider range of parameter values compared to earlier studies[1]).

As can be clearly seen, the above scaling form (1a) reduces to a power law $A\sim h_0^a\omega^b T^{-c}$ with $a=\alpha-\epsilon\gamma$, $b=\epsilon$, and $c=\beta+\epsilon\delta$ in the $\omega\to 0$ limit. We thus get $a=0.70$, 0.67, and 0.32, $b=0.36$, 0.45, and 0.50, and $c=1.18$, 1.98, and 1.12 in $D=2$, 3, and 4, respectively

TABLE I. Exponent values for the best fit of the Monte Carlo data for A variation to the scaling form (1) in different dimensions. The same for mean-field results are also given.

D	α	β	γ	δ	ϵ
2	1.00	0.75	0.85	1.20	~0.36
	±0.02	±0.05	±0.05	±0.08	
3	1.00	1.20	0.70	1.75	~0.45
	±0.02	±0.03	±0.04	±0.08	
4	1.00	0.45	1.35	1.35	~0.50
	±0.02	±0.03	±0.05	±0.08	
MF	~1	~$\frac{1}{2}$	~$\frac{1}{2}$	~0	

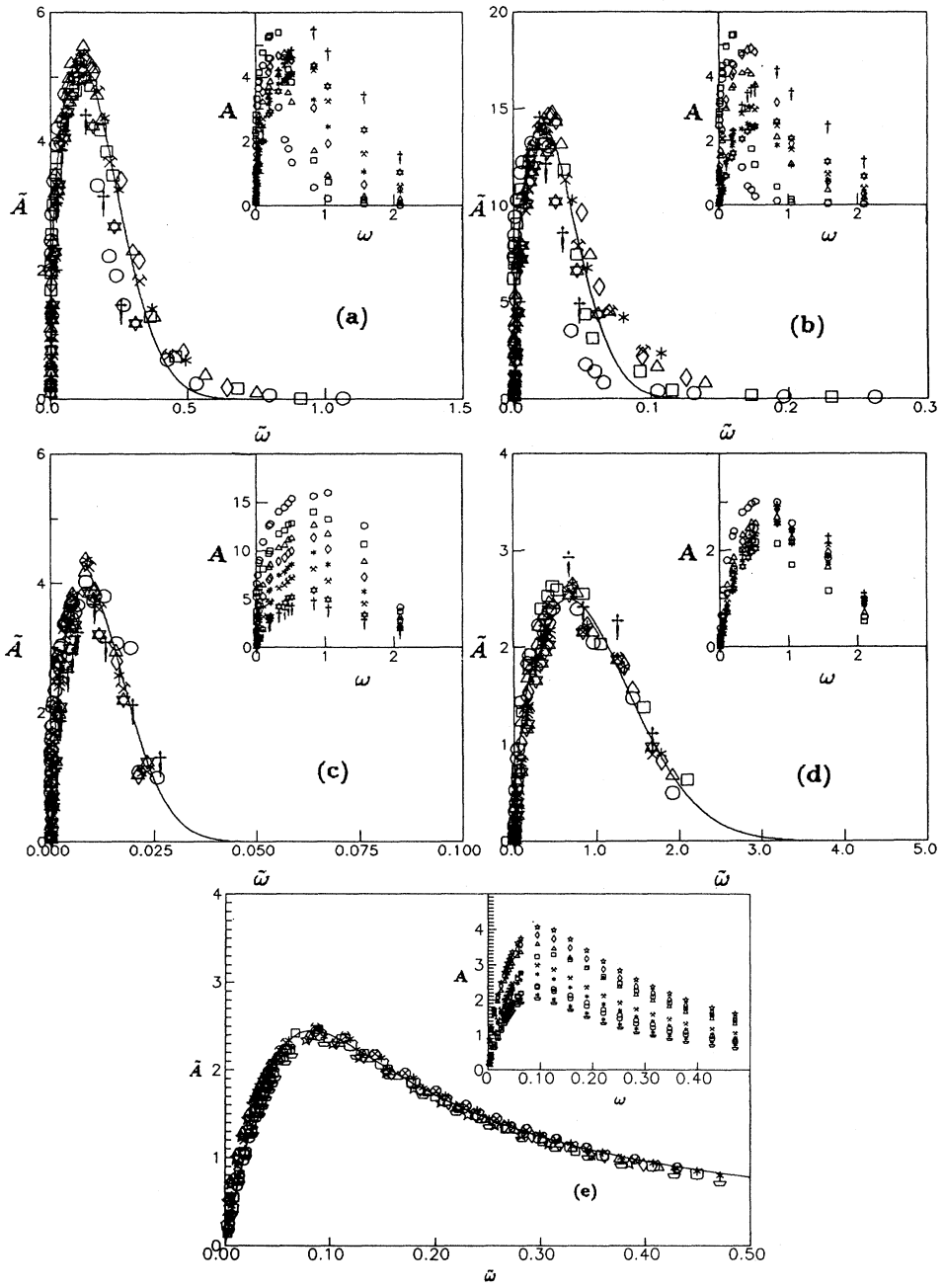

FIG. 2. Variation of scaled loop area $\tilde{A}=Ah_0^{-\alpha}T^{\beta}$ with the scaled frequency $\tilde{\omega}=\omega/h_0^{\gamma}T^{\delta}$. The inset shows the variation of A with ω at different h_0 and T. (a) For the MC data in $D=2$. Different symbols correspond to different T and h_0: ○, $T=1.5$, $h_0=1.25$; □ $T=1.5$, $h_0=1.5$; △, $T=2.0$, $h_0=1.25$; ◇ $T=2.0$, $h_0=1.5$; ∗, $T=2.5$, $h_0=1.5$; χ, $T=2.5$, $h_0=1.75$; ☆, $T=3.0$, $h_0=2.0$; and †, $T=3.0$, $h_0=2.5$. The solid curve indicates the proposed scaling function $g(x)\sim x^{\epsilon}\exp(-x^2/\sigma)$ and $\epsilon=0.36$. (b) For the MC data in $D=3$. Different symbols correspond to different T and h_0: ○, $T=3.0$, $h_0=1.25$; □, $T=3.0$, $h_0=1.5$; △, $T=4.0$, $h_0=1.5$; ◇, $T=4.0$, $h_0=1.75$; ∗, $T=5.0$, $h_0=1.25$; χ, $T=5.0$, $h_0=1.5$; ☆, $T=6.0$, $h_0=1.75$; and †, $T=6.0$, $h_0=2.5$. The solid curve indicates the proposed scaling function $g(x)\sim x^{\epsilon}\exp(-x^2/\sigma)$ and $\epsilon=0.45$. (c) For the MC data in $D=4$. Different symbols correspond to different T and h_0: ○, $T=4.0$, $h_0=6.5$; □, $T=5.0$, $h_0=6.0$; △, $T=5.5$, $h_0=5.5$; ◇, $T=6.0$, $h_0=5.0$; ∗, $T=6.5$, $h_0=4.5$; χ, $T=7.0$, $h_0=4.0$; ☆, $T=8.0$, $h_0=3.5$; and †, $T=8.5$, $h_0=3.0$. The solid curve indicates the proposed scaling function $g(x)\sim x^{\epsilon}\exp(-x'2/\sigma)$ and $\epsilon=0.50$. (d) For the MC data in $D=1$. Different symbols correspond to different T and h_0: ○, $T=1.0$, $h_0=1.25$; □, $T=1.25$, $h_0=1.0$; △, $T=1.25$, $h_0=1.25$; ◇, $T=1.5$, $h_0=1.5$; ∗, $T=1.75$, $h_0=1.5$; χ, $T=1.75$, $h_0=1.75$; ☆, $T=2.0$, $h_0=1.75$; and †, $T=2.0$, $h_0=2.0$. The solid curve indicates the proposed scaling function $g(x)\sim x^{\epsilon}\exp(-x^2/\sigma)$ and $\epsilon=0.50$. (e) For the MF data. Different symbols correspond to different T and h_0: ○, $T=1.5$, $h_0=1.2$; □, $T=2.25$, $h_0=2.0$; △, $T=0.75$, $h_0=1.3$; ◇, $T=0.75$, $h_0=1.4$; ☆, $T=0.75$, $h_0=1.5$; ∗, $T=1.0$, $h_0=1.1$; χ, $T=1.0$, $h_0=1.2$; ⛤, $T=1.25$, $h_0=1.0$; and ⛛, $T=1.25$, $h_0=1.1$. The solid line indicates the proposed scaling function $g(x)\sim x/[1+(cx)^2]$.

(from Table I). These values for a and b agree well with the previous Monte Carlo[8] and cell dynamical[9] estimates for the previously estimated values of a and b in $D=2$.

In Fig. 2(a), we show the results of the scaling fit in two dimensions ($L=100$). The range of the temperature (T) was from 1.5 to 3.0 and that of the field amplitude (h_0) was from 1.25 to 2.5. In $D=3$, as mentioned before, we have taken $L=20$ and studied the variation of A with ω for various temperatures ($T=3.0$, 4.0, 5.0, 6.0) and field amplitudes (h_0 ranging from 1.25 to 2.5); see Fig. 2(b). In $D=4$ we have taken $L=10$ and the variation in A with ω at different T (in the range from 4.0 to 8.5) and for h_0 ranging from 3.0 to 6.5 [Fig. 2(c)]. Similar results for $D=1$ ($L=10\,000$) is shown in Fig. 2(d). In all these figures, we show the original data for variations of A with ω at different h_0 and T in the corresponding insets. The figures themselves show the best fit to the scaling form (1a).

We have also estimated the area of the m-h loop (hysteresis loop) obtained from the solution of the mean-field equation of motion (3) for various values of ω, h_0, and T. We tried to fit all these results for $A(\omega,h_0,T)$ to the scaling form (1) and the best fit was obtained [see Fig. 2(e)] with a Lorentzian scaling function (1b). The best-fit values for the exponents α, β, γ, and δ are around 1, $\frac{1}{2}$, $\frac{1}{2}$, and 0, respectively. In the $\omega\to 0$ limit above relation (1b) reduces to the power law (and putting above values of α, β, γ, δ, and ϵ) and we get $a\cong\frac{1}{2}$, $b\cong 1$, and $c\cong\frac{1}{2}$ in MF approximation. In fact, in the linearized limit ($h_0\to 0$ and large T), the mean-field equation of motion (3) can be solved and integrated to give (see the Appendix)

$$\begin{aligned} m(t)&=m_0\cos(\omega t-\phi)\ , \\ m_0&=h_0/T[\epsilon^2+(\omega^2\tau^2)]^{1/2}\ , \\ \phi&\equiv\omega\tau_{\rm eff}=\sin^{-1}\{\omega\tau/[\epsilon^2+(\omega^2\tau^2)]^{1/2}\}\ , \end{aligned} \tag{5}$$

for the stable solution. The response of a sinusoidally varying field is thus also a similarly (time)-varying magnetization with the same frequency but with a phase lag ϕ. The Lissajous plot of $m(t)$ versus $h(t)$ will enclose some nonzero area if the ϕ is nonzero. The phase lag (ϕ) of the response (magnetization) compared with that of the perturbing field is determined by the finite relaxation time τ/ϵ ($\phi=0$ for $\tau/\epsilon=0$), and hysteresis loss is finite (area is nonzero) where ϕ is nonzero. In this linearized case, one can calculate the area of the (stabilized) hysteresis loop

$$A=\oint m\,dh\sim\frac{h_0^2\omega\tau}{T[\epsilon^2+(\omega^2\tau^2)]}\ . \tag{6}$$

This gives the Lorentzian form (1b) mentioned above, for the scaling function $g(x)$. In fact, it is quite interesting to note that this same Lorentzian form of A remains valid more generally (even when linearization cannot be done), and this can be seen from the Lorentzian fit [Fig. 2(e)] of the scaling function $g(x)$ for the numerical solutions of the loop area A obtained from the solution of Eq. (3). However, it may be noted that the values of the exponents α, β, γ, and δ [in Eq. (1)] are different from those in this linear limit.

D. Dynamic transition

The other important and interesting aspect of such hysteretic response is the dynamic phase transition,[1,3] first indicated in the mean-field solution of the dynamic response.[3] If the Ising system is placed in a sinusoidally varying longitudinal magnetic field, the time-averaged magnetization over a complete cycle [$\oint m(t)dt=Q$, normalized over the time period $2\pi/\omega$ of the oscillating field] acquires a nonzero value in the low field (amplitude) and temperature region in the h_0-T plane, separated by a phase boundary $T_d(h_0,\omega)$. The mean-field solution also indicated the existence of a tricritical point [$T_d^{\rm TCP}(h_0,\omega)$] on the phase separation line, across which the nature of the transition crosses over from discontinuous to a continuous one.

The observed phase separation line (separating the $Q\neq 0$ phase from the $Q=0$ phase) is shown in Figs. 3(a)–3(c) for the Monte Carlo studies in $D=1$, 2, and 3, respectively. In two dimensions, the MC data shown in Fig. 3(b) are for $L=100$ and we studied the variation of the phase separation line $T_d(h_0,\omega)$ for different ω. We find that as the frequency decreases, the phase boundary line (T_d line) shrinks inward in the h_0-T plane. We also find that the crossover of this transition across $T_d(h_0,\omega)$, from a discontinuous to a continuous one, at $T_d^{\rm TCP}(h_0,\omega)$, is very prominent [see inset of Fig. 3(b), showing the nature of the transition just below and above the TCP at a particular ω]. Here, in two and three dimensions, the tricritical point is observed to be more or less independent of frequency [Figs. 3(b) and 3(c)]. However, in one dimension the tricritical point clearly depends on frequency [see Fig. 3(a)]. Here also the phase separation lines are shown for different frequencies ($\omega=0.208$, 0.104, 0.052), obtained from the MC study for $L=1000$. The crossover at the tricritical point is again very prominent as shown in the inset of Fig. 3(a), where the nature of the transition just below and above the TCP at $\omega=0.104$ is given. We observed similar behavior of the dynamic phase transition in $d=3$ [Fig. 3(c)]. The mean-field results for the dynamic transition are shown in Fig. 3(d). Although the dynamic transition exists for the solution of the mean-field equation of motion [Fig. 3(d)], the existence of the transition in the Monte Carlo case (in the presence of fluctuations) has been checked using a finite-size variation study. In Fig. 4(a) we show the variation of Q (at fixed $h_0=2.0$, $\omega=0.104$, and $T=1.5$) with $1/L$ (for L varying from 10 to 100) for $D=3$. No significant finite-size effect is observed. Figure 4(b) shows that as the frequency decreases, the limiting zero-field dynamic transition point T_d^0 [where the T_d line cuts the T axis in the h_0-T plane in, e.g., Figs. 3(a)–3(c)] approaches the ordering temperature T_c ($=0$, 2.27, and 4.51 in $D=1$, 2, and 3, respectively) for the ferromagnetic-paramagnetic transition (in the absence of any external magnetic field).

The dynamic phase transition is, in fact, a manifestation of the coercivity property (one of the important features of hysteresis). In the $Q\neq 0$ phase, the m-h loop is not symmetric about the field axis and lies in the upper half (or lower half) of the m-h plane depending on the initial magnetization. Even in the static limit, a minimum

magnitude of external and opposite magnetic field (coercive field) is required to change the sign of the magnetization for complete spin reversal. This magnitude of the coercive field depends on the temperature T. The coercive field increases as the temperature decreases. In the case of a sinusoidally varying field, for a transition to a $Q=0$ phase from a $Q\neq 0$ phase, the field amplitude should be at least of the order of the coercive field depending upon the temperature. So, in a sense, the phase boundary for the dynamic phase transition (in the low-field limit) is the coercive field variation with respect to temperature. Since $h(t)=h_0\cos(\omega t)$ and $|h(t)|\leq h_0$, the phase boundary is the upper bound of the coercive field variation with respect to temperature. However, the difference of this upper bound increases with increasing frequency, because of the effective relaxation lag. In fact, the tricritical point $T_d^{\rm TCP}(h_0,\omega)$ on the phase boundary appears because of the failure to relax within the time period ($=2\pi/\omega$) of the external field. The intrinsic relaxation time in the ferromagnetic phase decreases with lowering of the temperature and below $T_d^{\rm TCP}(h_0,\omega)$, $\tau_{\rm eff}\leq 2\pi/\omega$ (equality at $T=T_d^{\rm TCP}$), so that the magnetization changes sign (from m to $-m$) abruptly and consequently Q changes from a value very near unity to 0 discontinuously. This indicates that $T_d^{\rm TCP}$ should decrease with higher frequency as is indeed observed [see, e.g., the inset of Fig. 3(d) for MF result]. In fact, at zero temperature, the transition is completely mechanical (purely field driven, without any thermal fluctuation) and

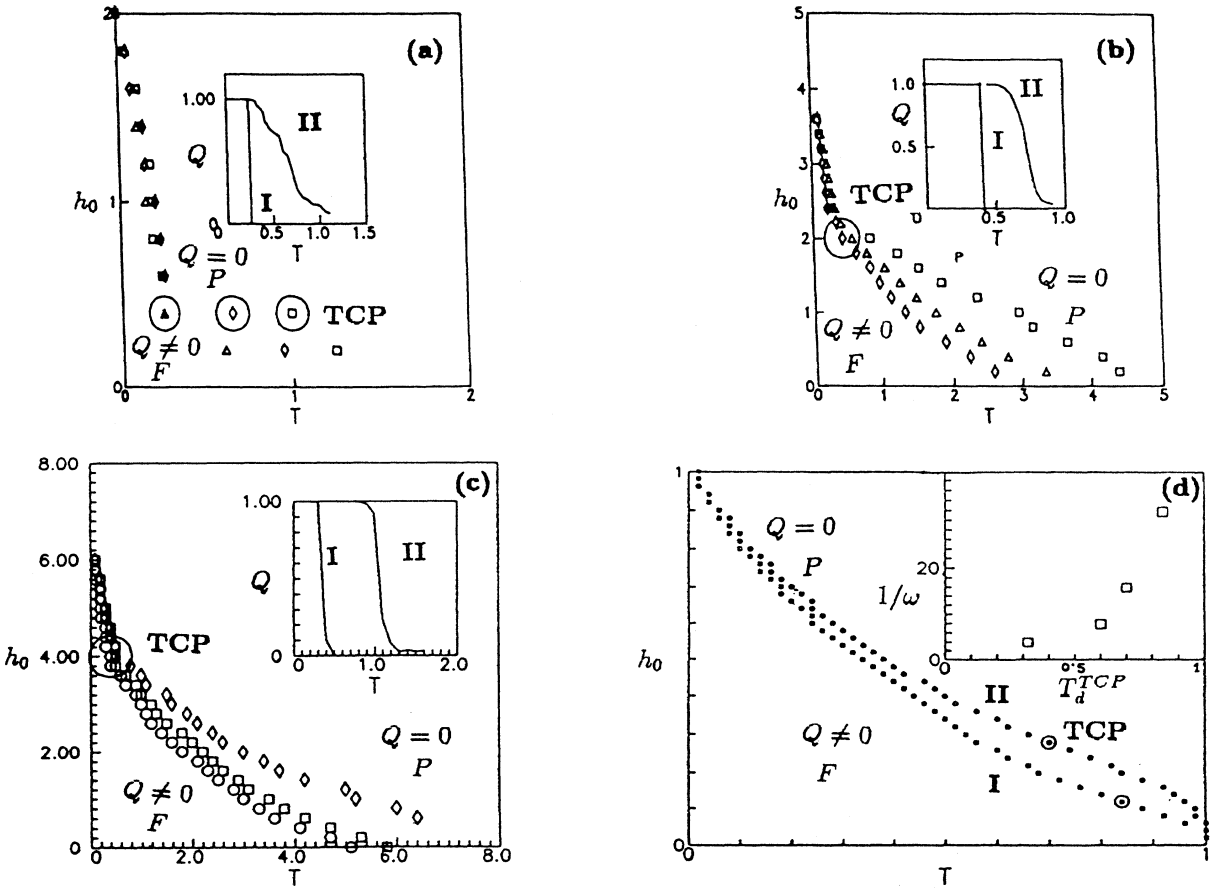

FIG. 3. Phase diagram $T_d(h_0,\omega)$ for the dynamic phase transition: below $T_d(h_0,\omega)$, Q acquires a nonzero value in the F phase and $Q=0$ in the P phase. Different symbols denote different phase boundary lines corresponding to different frequencies (ω). (a) Monte Carlo results in $D=1$. □, $\omega=0.208$; △, $\omega=0.104$; and ◇, $\omega=0.052$. The location of tricritical points (TCP) is indicated by the circles. Inset shows the nature of the transition just above (I: $h_0=0.8$) and below (II: $h_0=0.3$) the tricritical point along the phase boundary. (b) Monte Carlo results in $D=2$. □, $\omega=0.418$; △, $\omega=0.208$; and ◇, $\omega=0.104$. The location of the TCP is indicated by the circle. Inset shows the nature of the transition just above (I: $h_0=2.2$) and below (II: $h_0=1.8$) the tricritical point along the phase boundary. (c) Monte Carlo results in $D=3$. ◇, $\omega=0.418$; □, $\omega=0.208$; and ○, $\omega=0.104$. The location of the TCP is indicated by the circle. The inset shows the nature of the transition above (I: $h_0=4.4$) and below (II: $h_0=3.6$) the tricritical point along the phase boundary. (d) Mean-field results. (I) $\omega=0.012$ and (II) $\omega=0.025$. The locations of the tricritical points (different frequencies) are indicated by the circles. The inset shows the variation of the location of the tricritical points $T_d^{\rm TCP}$ with respect to $1/\omega$.

can only be a discontinuous one. Above $T_d^{\rm TCP}$, the thermal fluctuations win over and determine the nature of the transition.

Although the appearance of the dynamic transition is due to the breakdown of linear approximation in, say, the solution of mean-field Eq. (3), we will show in what follows that a linear analysis or solution [of the form (5)] with an additional additive constant (with nonzero value inside the $Q\neq 0$ phase and vanishing for $Q=0$) will still suffice for the understanding of the nature of the transition (see next section).

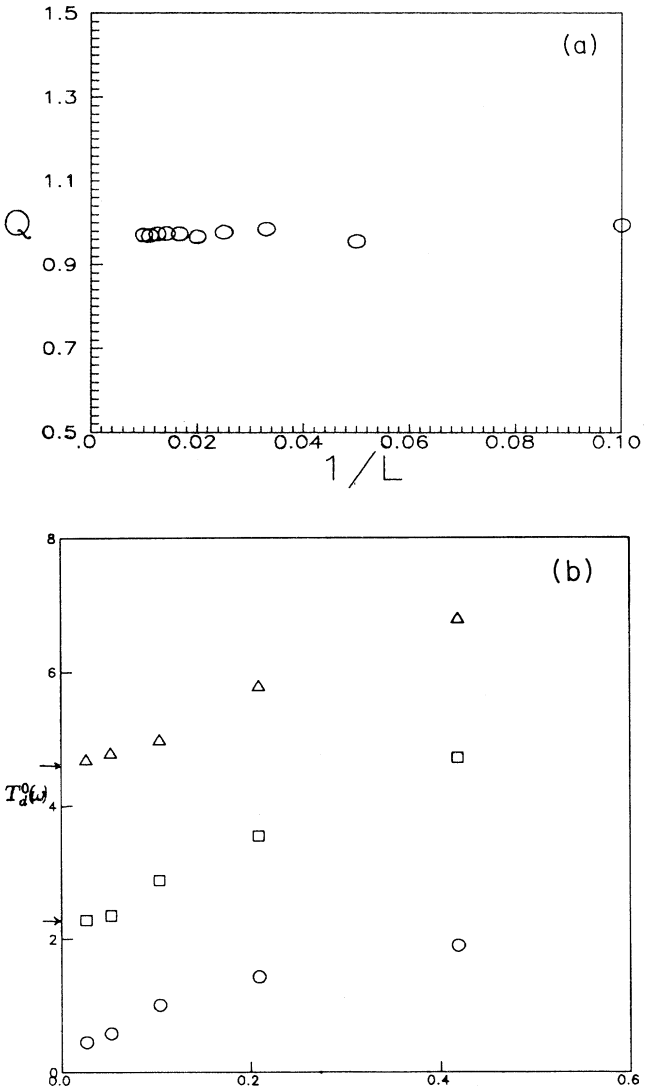

FIG. 4. (a) Checking of the finite-size effect in the dynamic transition in MC studies in $D=3$. We plot the Q values (at fixed $h_0=2.0$, $\omega=0.104$, and $T=1.5$) against $1/L$ ($10\leq L\leq 100$). (b) Variation of the limiting zero-field dynamic tricritical point T_d^0 with frequency ω. ○ corresponds to $D=1$; □ corresponds to $D=2$; and △ corresponds to $D=3$. The horizontal arrows indicate the T_c's (for $h_0=0$) in $d=2$ and 3.

E. ac susceptibility

ac susceptibility measurements are now commonly used to determine magnetic and superconducting properties of materials.[14,15] Typically, in an electrically conducting (magnetic or superconducting) material, if the external magnetic field (h) is periodically varied (say sinusoidally) in time (t), then the induced eddy current,[16] in turn, produces a response magnetization $m(t)$ given by a complex susceptibility (χ) having both the real or in-phase (χ') and the imaginary or loss or out-of-phase (χ'') parts. The m-h plot also gives the hysteresislike loops with finite area (giving typically very small eddy loss) as the χ'' is nonvanishing. The temperature and frequency variation of the hysteresis loss or of χ'' (coming from the temperature variation of the conductivity of the sample[15]) are then studied[14] to locate the transition point of the (electrical) conductivity of the (superconducting) samples. There are also comparatively older reports[14] on such properties of χ'' (and χ') in magnetic materials. The above-mentioned out-of-phase part (χ'') of the susceptibility and the consequent hysteresis loss (in conducting magnets) arise due to the delayed response [magnetization $m(t)=m_0\cos(\omega t-\phi)$; $\chi''=(m_0/h_0)\sin(\phi)$] to the external field variation [$h(t)=h_0\cos(\omega t)$]. This loss originates from the nature of the induced eddy currents,[16] or from the laws of electrodynamics (giving always linear response, which is noncooperative in nature).

Here, we study the thermodynamic ac susceptibility of cooperatively interacting Ising systems,[13] using both MC and MF dynamics (which are generally nonlinear). As discussed in Sec. II B, the magnetic response of an Ising system in a sinusoidally varying external field can be expressed as Eq. (4): $m(t)=P(\omega(t-\tau_{\rm eff}))$ with an effective amplitude $m_0(h_0,T,\omega)$. Let us define here also the (linear) ac susceptibility as

$$\chi=(m_0/h_0)e^{-i\phi},\quad \phi=\omega\tau_{\rm eff}\ ,$$

or

$$\chi'=(m_0/h_0)\cos(\omega\tau_{\rm eff})\ ,\qquad \chi''=(m_0/h_0)\sin(\omega\tau_{\rm eff})\ . \tag{7}$$

We have measured χ' and χ'' from the numerical estimate of $\tau_{\rm eff}$ (from the difference between the minima positions of magnetization and magnetic field). The solution of the mean-field equation [Eq. (3)] for χ' and χ'' is shown in Fig. 5(a) where we also show (for comparison) the variation of the response amplitude m_0 and order parameter $Q(=\oint m dt)$ for the dynamic phase transition. In Figs. 5(b) and 5(c), the same are shown for Monte Carlo dynamics of $D=2$ and 3 (sizes 100^2 and 20^3, respectively, averaging over 200 Monte Carlo seed values) Ising system. One can identify the high-temperature smeared peak in χ' with the high-temperature decay of magnetization amplitude (m_0) and the second (low-temperature) prominent peak in χ'' (and the dip in χ') with the dynamic transition (Q changing from a zero to a nonzero value). A similar behavior for χ' and χ'' is shown in Fig. 5(a), as obtained from the numerical solution of the mean-field equation of motion (3), using the fourth-order Runge-

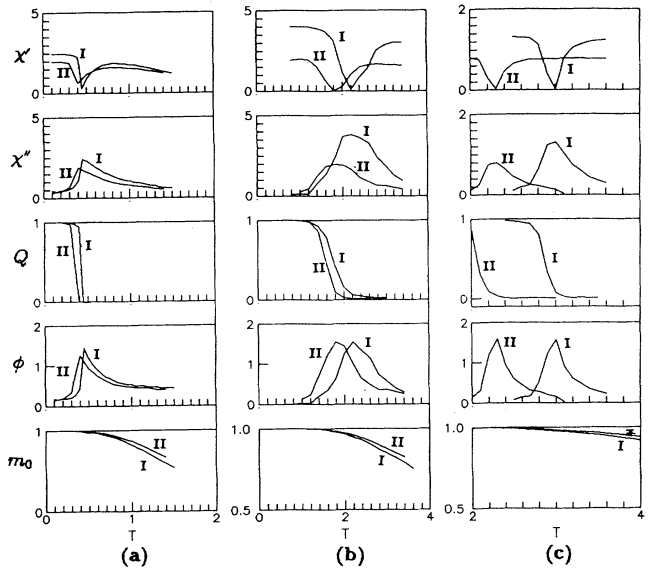

FIG. 5. Temperature variations of χ', χ'', Q, ϕ, and m_0 for two different field amplitudes (h_0). (a) Mean-field case: I: $h_0=0.4$, $\omega=0.031$, and II: $h_0=0.5$, $\omega=0.031$. (b) Monte Carlo results in $D=2$: I: $h_0=0.5$, $\omega=0.125$; II: $h_0=0.8$, $\omega=0.125$. (c) Monte Carlo results in $D=3$: I: $h_0=0.75$, $\omega=0.125$; II: $h_0=1.25$, $\omega=0.125$.

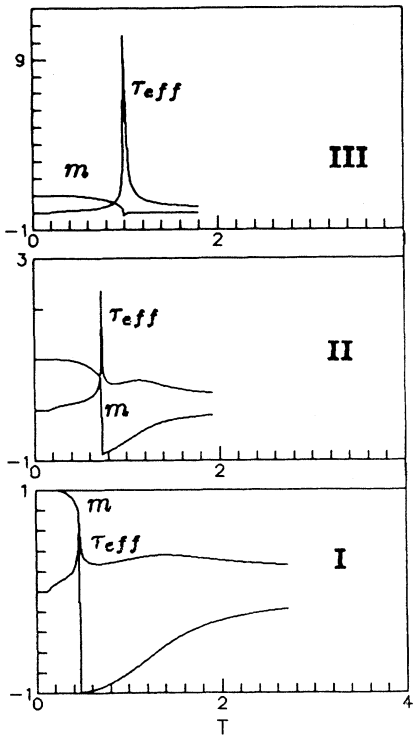

FIG. 6. Behavior of the effective relaxation time (τ_{eff} for static field) and equilibrium magnetization with respect to temperature in the presence of a static negative field (in the mean-field case): I: $h_0=-0.3$; II: $h_0=-0.1$; III: $h_0=-0.001$. Initial magnetization was $+1$ in all cases.

Kutta scheme.

The linearized theory, as discussed above, can easily account for such (observed) variations in the mean-field case. These observations for frequency dependence of χ' and χ'' are also very much comparable to those observed in conducting magnets.[14] As shown in Sec. II C, the solution can be written as $m(t)=m_0\cos(\omega t-\phi)$, where $m_0=h_0/(\epsilon^2+\omega^2\tau^2)^{1/2}T$ and $\phi=\sin^{-1}[\omega\tau/(\epsilon^2+\omega^2\tau^2)^{1/2}]$. One can then express the complex susceptibility as $\chi'=(m_0/h_0)\cos(\phi)$ and $\chi''=(m_0/h_0)\sin(\phi)$.

This peak (dip) in χ'' (χ') at the dynamic transition point thus comes from the corresponding peak in τ_{eff} or the phase lag ϕ (with the variation of temperature). This dominant peak in τ_{eff} (slowing down of relaxation) comes from the almost discontinuous (nearly first-order) transition where the external field goes above the coercive field and a spin-reversal domain is quite abruptly formed (for $\omega\neq0$; exact discontinuity at $\omega=0$). To see this we studied the relaxation behavior of the mean-field system in the presence of a static field $-h_0$ [$\omega=0$ in Eq. (3)] opposite to the orientation of the initial magnetization (we start with $m=\pm1$ at $t=0$). The relaxation time has two peaks; one is very sharp and the other is quite smeared (see Fig. 6). The sharp peak indicates the temperature at which the applied negative static field becomes comparable with the coercive field [where the magnetization discontinuously jumps from $+m(t)$ to $-m(t)$]. Thus, in the presence of oscillating field at a certain value of the amplitude which is sufficient (at that temperature) to provide for the coercive field, the dynamic transition occurs. For that temperature, the effective time lag will be max-

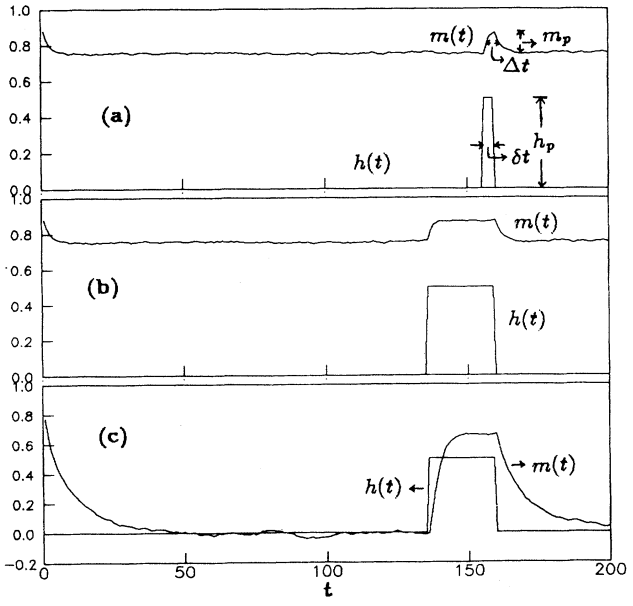

FIG. 7. Time variations of the response magnetization $m(t)$ and the pulse field $h(t)$ for the Monte Carlo study in $D=3$. (a) $T=4.0$, $\delta t=5$ MCS's, and $h_p=0.5$. (b) $T=4.0$, $\delta t=25$ MCS's, and $h_p=0.5$. (c) $T=5.0$, $\delta t=25$ MCS's, and $h_p=0.5$.

imum and consequently the phase lag ϕ will be maximum. At that point χ'' will give a peak and χ' will give a dip. After that, χ' will again tend to grow but with increasing temperature, the amplitude m_0 starts falling, and consequently, χ' shows a smeared peak at an optimal temperature ($T>1$).

Our study on the temperature variation of the complex susceptibility of an Ising model in a periodically varying external field shows that a low-temperature prominent peak in χ'' (and dip in χ') occurs (at T_d) as one crosses the dynamic phase boundary [$Q\neq 0$ for $T<T_d(h_0,\omega)$ and $Q=0$ for $T\geq T_d$]. In fact, this observation of a sharp peak (dip) in the ac susceptibility across the dynamic transition line indicates the dynamic transition to be a truly thermodynamic transition. This is also supported by the observation (see Fig. 4) that the limiting transition temperature T_d^0 (for $h_0\to 0$) approaches the order-disorder transition temperature T_c as $\omega\to 0$. The experimental measurements of the behavior of χ'' in magnetic insulators would thus be able to detect the intriguing dynamic phase transition (and determine the phase boundary).

F. Behavior of the response due to a pulsed magnetic field

In order to investigate another interesting dynamic response of such systems, we have studied the response of a pulsed magnetic field both by Monte Carlo simulation and also by solving the dynamical equation of motion for the response magnetization in the mean-field approximation. Here, the time variation of the external field has been taken as

$$h(t)=h_p \quad \text{for } t_0<t<t_0+\delta t\ , \qquad =0, \quad \text{elsewhere}\ . \tag{8}$$

In both the cases, we have first allowed the system to relax from a nonequilibrium state ($m=1, T\neq 0$) to its equilibrium state at any nonzero temperature (T), and then applied the pulse for a short duration δt (compared with the relaxation time). As the pulse has been applied, the response magnetization gets sharply peaked over its equilibrium value. This response (see, e.g., Fig. 7) is characterized by two quantities: the height m_p and its half-width Δt of the pulsed response magnetization $m(t)$ (over its equilibrium value). We thus measure two important quantities: (i) width ratio $R=\Delta t/\delta t$ and the pulse susceptibility $\chi^p=m_p/h_p$. We have studied the temperature variation of R and χ^p. In the MC case in the $D=2$ Ising system, we have taken $h_p=0.25$, $\delta t=5$ Monte Carlo steps (MCS's) and the system size is $L=500$. R shows a sharp peak and χ^p shows a smeared peak near $T\cong 2.6$ [at somewhat higher T than T_c (Onsager) $\cong 2.69$] [Fig. 8(a)]. In $D=3$ the system size is $L=100$, pulse (field) height $h_p=0.5$, and the pulse width $\delta t=5$ MCS. Here, the corresponding peaks of R and χ^p have been observed near $T\cong 4.6$ (slightly higher than $T_c\cong 4.511$) [Fig. 8(b)]. In the MF case the corresponding sharp peaks have been observed at $T\cong 1.001$ [for $h_p=0.01$, $\delta t=50$ times the time differential for solving the MF equation; T_c

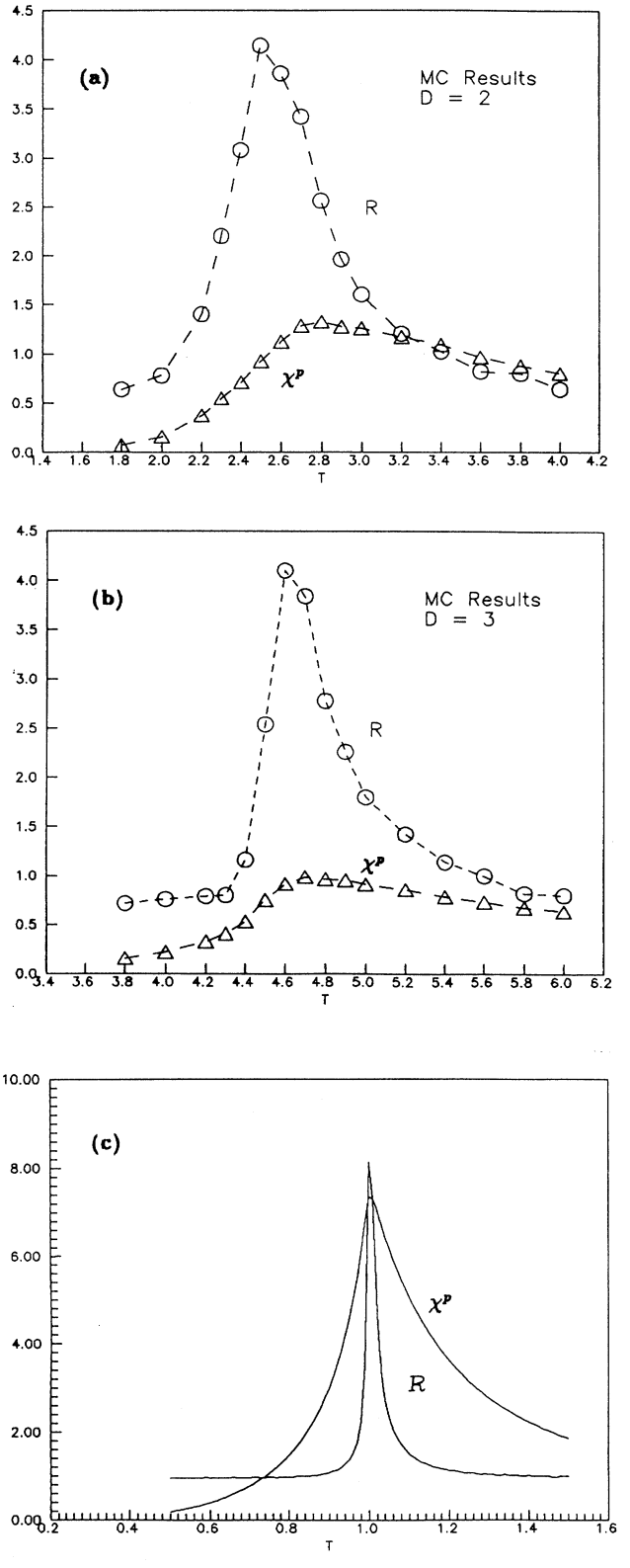

FIG. 8. Temperature (T) variation of width ratio R and χ^p. (a) Monte Carlo case in $D=2$; $L=500$, $h_p=0.25$, $\delta t=5$ MCS's. (b) Monte Carlo case in $D=3$; $L=50$, $h_p=0.5$, $\delta t=5$ MCS's. (c) Mean-field case; $h_p=0.01$, $\delta t=50x\ dt$.

(MF)=1] [Fig. 8(c)]. In all these cases, the effective T_c obtained from the peak position is slightly overestimated, and this overestimation disappears in the limit $h_p \to 0$ and $\delta t \to 0$. It may also be mentioned that $\chi^p \to \chi$, the static susceptibility, in the limit $h_p \to 0$, $\delta t \to \infty$. Also, the sharpness of the peak in the MF case, and the increasing sharpness and height of the peak with the system size (L) in the MC cases, indicate the divergence of χ^p and R at the order-disorder transition point.

Since short pulses do not affect significantly the static equilibrium transitions of the system and yet can sense the critical fluctuations of the equilibrium (static) phase, as can be seen in the above study of the pulse susceptibility and width ratios, etc., the pulse response studies of self-organized or self-tuned systems (where the phase transition point cannot be tuned externally; often a catastrophic point) can give prior indications of an imminent transition point. One can consider, for example, the study of acoustic pulse response (susceptibility/width ratio) in a system with propagating or spreading rupture/fracture.[19] An increasing tendency of the width ratio here can indeed give the prior indication of the catastrophe.

III. RESPONSE OF ISING SYSTEMS IN THE PRESENCE OF TIME-VARYING TRANSVERSE FIELD

A. Model Hamiltonian and the mean-field equation of motion

We consider a ferromagnetically interacting Ising system placed, in general, in time-dependent transverse as well as axial (or longitudinal) field. The general system can thus be described by the model Hamiltonian

$$H = -\sum_{\langle i,j \rangle} J_{ij}\sigma_i^z\sigma_j^z - h(t)\sum_i \sigma_i^z - \Gamma(t)\sum_i \sigma_i^x , \tag{9}$$

where σ are the Pauli spin matrices, $\Gamma(t)$ represents the time-varying transverse field, $h(t)$ represents the time-varying longitudinal field, and J_{ij} are ferromagnetic spin-spin interaction strengths. The above Hamiltonian generally represents a cooperative asymmetrical double-well system, where both the tunneling (between the wells) term (Γ) and the (double-well) asymmetry term (h) are time dependent. In view of the wide applicability of the (time-dependent) transverse Ising Hamiltonian to represent the (tunneling-induced) order-disorder transition in hydrogen-bonded (potassium dihydrogenphosphate-type) ferroelectrics and Jahn-Teller compounds[17,20] and the possibility of tuning the asymmetry of the double-well (h) and the transverse (tunneling) field (Γ) by changing the external pressure on the hydrogen-bonded ferroelectrics,[20] etc., the study of quantum relaxation and hysteresis in such transverse Ising systems is not just of pedagogic interest. By suitable tuning of external parameters (e.g., tuning of transverse field by pressure modulation in order-disorder ferroelectrics), the interesting features of the dynamic response and hysteresis in such systems, as obtained here, can be studied.

Some interesting limits of the above Hamiltonian are (a) $h(t)=0$, $\Gamma(t)=\Gamma_0\cos(\omega t)$, (b) $h(t)=h_0\cos(\omega t)$, $\Gamma(t)=\Gamma(\text{const})$, and (c) $h(t)=0$, $\Gamma(t)=\Gamma+\delta\Gamma$ for $t_0 < t < t_0+\delta t$ and $\Gamma(t)=\Gamma$, otherwise. The first case had been studied earlier.[10] The other two cases are investigated and reported here in detail.

In the mean-field approximation, the effective molecular field can be approximated as

$$\mathbf{h} \cong [m^z + h(t)]\hat{z} + \Gamma(t)\hat{x} ,$$

so that the Hamiltonian takes the form

$$H = \sum_i \mathbf{h}\cdot\boldsymbol{\sigma}_i . \tag{10}$$

Here again, the nearest-neighbor sum over J_{ij} has been taken to be unity. The generalized mean-field equation of motion for the average magnetization can then be written as[10]

$$\tau\frac{d\mathbf{m}}{dt} = -\mathbf{m} + \left[\tanh\left[\frac{|h|}{T}\right]\right]\frac{\mathbf{h}}{|h|} ,$$
$$|h| = \sqrt{\{[m^z + h(t)]^2 + \Gamma(t)^2\}} . \tag{11}$$

It may be mentioned here that the microscopic relaxation time τ can, in principle, differ for longitudinal and transverse magnetization. In order to reduce the number of free parameters in the Hamiltonian, we have considered them identical here. In the classical limit ($\Gamma=0$), the above equation of motion reduces to the well-known mean-field equation (see Sec. II A) for the Ising dynamics in the presence of an oscillating longitudinal field.

B. Response magnetization and the dynamic transition behavior for oscillating transverse field (with zero longitudinal field)

Here, the axial or longitudinal field is zero [$h(t)=0$] and the transverse field is sinusoidally varying in time, i.e., $\Gamma(t)=\Gamma_0\cos(\omega t)$. This case has been considered by ACS,[10] who studied extensively the hysteretic response and the dynamic phase transition. We summarize here the important results obtained for this special case [case (a)] represented by the Hamiltonian

$$H = -\sum_{\langle ij \rangle} J_{ij}\sigma^z{}_i\sigma^z{}_j - \Gamma(t)\sum_i \sigma^x{}_i ,$$
$$\Gamma(t) = \Gamma_0\cos(\omega t) , \tag{12}$$

where σ are the Pauli matrices.

Using the mean-field equation of motion (11) in the case with $h(t)=0$, ACS[10] had already studied the variation of the longitudinal and transverse magnetization loop areas $A_x = \oint m^x d\Gamma$ and $A_z = \oint m^z d\Gamma$, respectively, and the dynamic order parameter $Q_z = \oint m^z dt$, as functions of the frequency (ω) and amplitude (Γ_0) of the periodically varying transverse field and the temperature (T) of the system. This had been done by solving the mean-field equations (11) of motion for the average magnetization $\mathbf{m} = \langle \boldsymbol{\sigma}_i \rangle = m^x\hat{x} + m^z\hat{z}$. They found that the variation of the loop area A_x with frequency ω for

different parameters (Γ_0 and T) can be expressed in a scaling form

$$A_x \sim \Gamma_0^{\alpha'} T^{-\beta'} g\left[\frac{\omega}{\Gamma_0^{\gamma'} T^{\delta'}}\right], \tag{13}$$

with a Lorentzian scaling function

$$g(x) \sim \frac{x}{1+cx^2}. \tag{14}$$

The best-fit values for the exponents α', β', γ', and δ' were found to be around 1.75 ± 0.05, 0.50 ± 0.02, 0 ± 0.02, and 0 ± 0.02, respectively. The mean-field equation of motion was solved analytically in three different (linearized) limits giving (i) $\alpha'=2$, $\beta'=1$, $\gamma'=0$, and $\delta'=0$ in the high-temperature limit, (ii) $\alpha'=2$, $\beta'=0=\gamma'=\delta'$ in the low tunneling field amplitude limit, and (iii) $\alpha'=1$, $\beta'=0=\gamma'=\delta'$ in the (adiabatic) limit of very slowly varying transverse field, with the Lorentzian scaling function (14). These limiting results (of effectively linear analysis) for the exponent values give the useful bounds for the observed exponent values.

The dynamic phase transition from $Q_z=0$ (for high Γ_0 and T) to $Q_z\neq0$ (beyond critical values of Γ_0 and T)

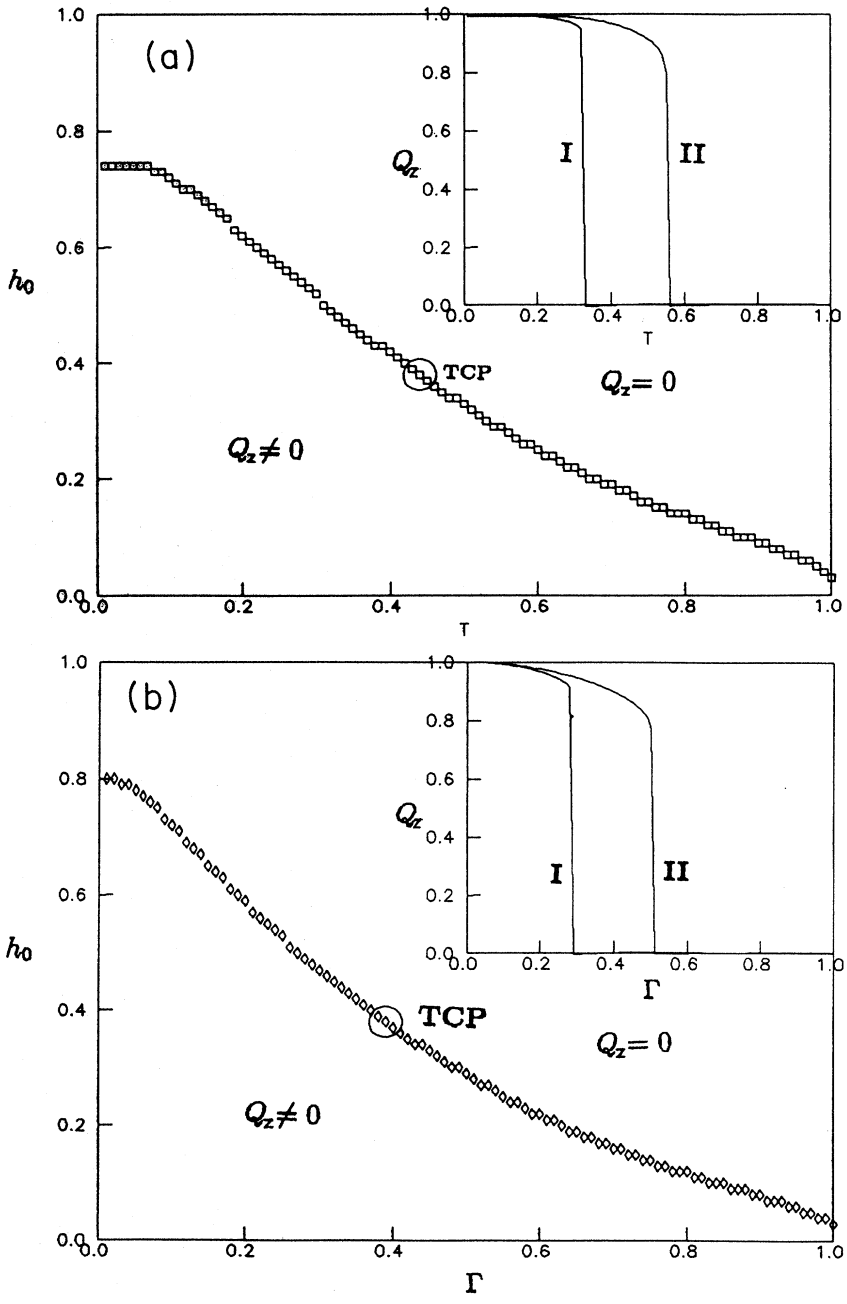

FIG. 9. (a) Projection of the dynamic phase boundary (and TCP) in the h_0-T plane. The inset shows the change of the nature of the dynamic transition just above (I: $h_0=0.48$) and below (II: $h_0=0.28$) the TCP. $\Gamma=0.2$ and $\omega=0.0314$ here. (b) Projection of the dynamic phase boundary (and TCP) in the h_0-Γ plane. The inset shows the change of the nature of the dynamic transition just above (I: $h_0=0.48$) and below (II: $h_0=0.28$) the TCP. $T=0.2$ and $\omega=0.0314$ here.

occurs across the Γ_0-T line and the phase diagram (in the Γ_0-T plane) for this transition had been obtained. An analytic estimate for the phase boundary line,

$$T=\tilde{\Gamma}_0/\sinh(\tilde{\Gamma}_0),\quad \tilde{\Gamma}_0=(\pi/2)\Gamma_0\ , \tag{15}$$

had been obtained, which gave a fair agreement with the numerical results.[10]

C. Numerical results for magnetization and dynamic transition behavior for oscillating longitudinal field (and static transverse field)

Let us consider the next case [case (b)], where Γ is constant, but $h(t)$ varies sinusoidally with time. Such a system is described by the Hamiltonian

$$H=\sum_{\langle ij\rangle} J_{ij}\sigma_i^z\sigma_j^z-\Gamma\sum\sigma_i^x-h(t)\sum\sigma_i^z\ ,$$
$$h(t)=h_0\cos(\omega t)\ . \tag{16}$$

We solved numerically the dynamical equation of motion (11) using a fourth-order Runge-Kutta method [in single precision; the value of the time differential (dt) was taken to be 10^{-6}]; the above (coupled) dynamical equations [for two components of magnetization in (11)] are self-consistently solved.

1. Dynamic phase transition

Using a simple trapezoidal rule we evaluated the dynamic order parameter $Q_z(=\oint m^z dt)$. For (classical) Ising systems, the dynamic phase transition has been extensively studied (see Sec. II D).

For the model considered here [represented by Hamiltonian (16)], where Γ is constant in time and $h(t)=h_0\cos(\omega t)$, there is a dynamic phase boundary $T_d(h_0,\omega,\Gamma)$ (separating the $Q_z\neq 0$ phase from the $Q_z=0$ phase). We find the projection of this boundary in the h_0-T plane for a fixed Γ and ω [Fig. 9(a)]. We also found a crossover of this transition across $T_d(h_0,\omega,\Gamma)$, from a discontinuous to a continuous one, at a tricritical point $T_d^{\rm TCP}(h_0;\omega,\Gamma)$; see inset of Fig. 9(a) showing the nature of the transition just below and above the TCP at a particular ω and Γ. Similar behavior of Q_z has been observed for other projections of the phase boundary. Figure 9(b) shows the phase boundary line $\Gamma_d(h_0,\omega,T)$ in the h_0-Γ plane (separating the $Q_z\neq 0$ phase from the $Q_z=0$ phase). The position of the tricritical point $\Gamma_d^{\rm TCP}(h_0,\omega,T)$ is also indicated on the phase boundary line. The inset of Fig. 9(b) shows the nature of the transition just below and above the TCP at a particular ω and T.

The dynamic phase transition, in fact, arises due to the coercivity property. In the $Q_z\neq 0$ phase, because of the failure of the external field to provide for the coercive field, the m-h loop is not symmetric about the field axis and lies in the upper half (or lower half) of the m-h plane depending upon the initial magnetization. So, the phase boundary equation $T_d(h_0,\omega,\Gamma)$ for the dynamic phase transition, when expressed as $h_0^d(T,\omega,\Gamma)$ gives in effect the coercive field variation with respect to T, Γ, and ω. The tricritical point $T_d^{\rm TCP}(h_0,\omega,\Gamma)$ appears because of

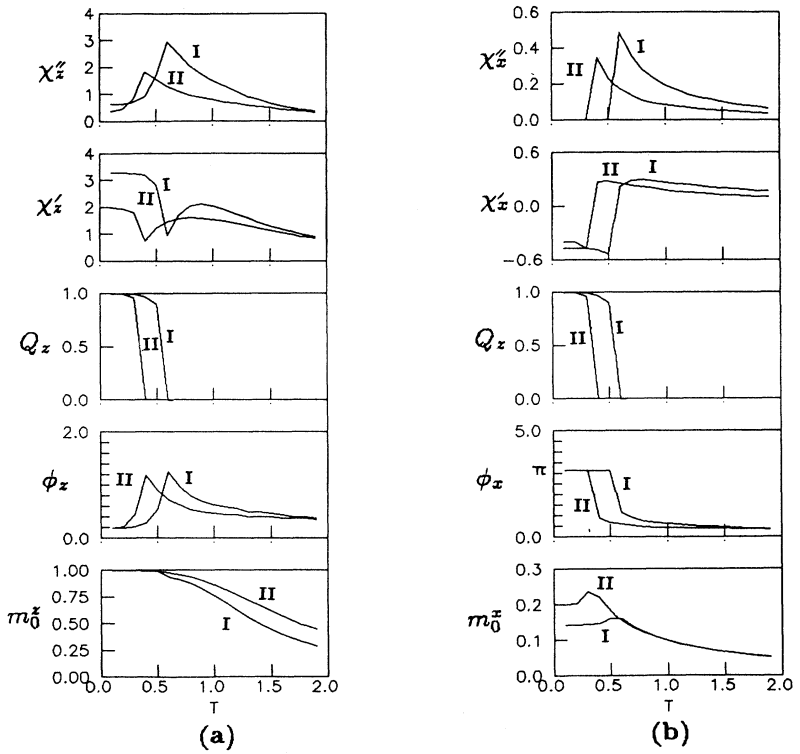

FIG. 10. (a) Temperature variation of χ_z', χ_z'', ϕ_z, Q_z, and m_0^z for two different values of h_0 and a fixed value of ω (0.0314) and Γ (=0.1). I: $h_0=0.3$ and II: $h_0=0.5$. (b) Temperature variation of χ_x', χ_x'', ϕ_x, Q_z, and m_0^x for two different values of h_0 and a fixed value of ω (0.0314) and Γ (=0.1). I: $h_0=0.3$ and II: $h_0=0.5$.

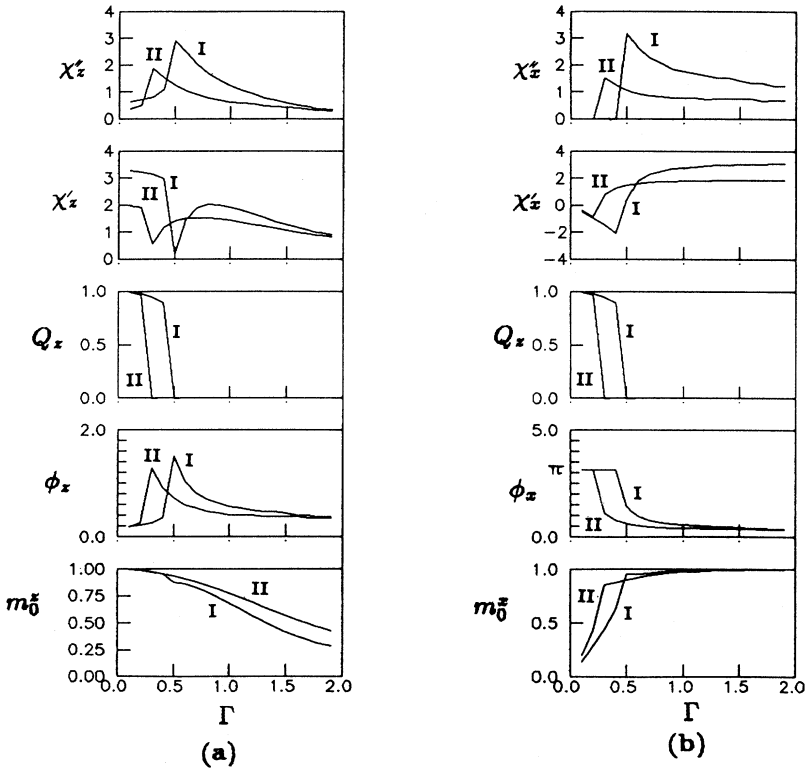

FIG. 11. (a) Γ variation of χ_z', χ_z'', ϕ_z, Q_z, and m_0^z for two different values of h_0 and a fixed value of ω (=0.0314) and T (=0.1). I: $h_0=0.3$ and II: $h_0=0.5$. (b) Γ variation of χ_x', χ_x'', ϕ_x, Q_z, and m_0^x for two different values of h_0 and a fixed value of ω (=0.0314) and T (=0.1). I: $h_0=0.3$ and II: $h_0=0.5$.

the failure of the system to relax within the time period $(2\pi/\omega)$ of the external field. The intrinsic relaxation time τ_{eff} in the ferromagnetic phase decreases with lowering of temperature and below $T_d^{\text{TCP}}(h_0,\omega,\Gamma)$: $\tau_{\text{eff}}(h_0,T)\leq 2\pi/\omega$ (equality at $T=T_d^{\text{TCP}}$), so that the magnetization changes sign (from m^z to $-m^z$) abruptly and consequently Q_z changes from a value very near unity to zero discontinuously. This indicates that $T_d^{\text{TCP}}(h_0,\omega,\Gamma)$ should decrease with increasing frequency, as has indeed been observed. The same is also true for $\Gamma_d^{\text{TCP}}(h_0,\omega,T)$.

2. *The* ac *susceptibility*

Following the successful introduction of ac susceptibility[13] for (classical) Ising systems, we study here the properties of similarly defined (linear) ac susceptibility in such a transverse Ising system.

In this case, by solving the mean-field equation of motion we obtained the time variation of m^x and m^z. Both the transverse and longitudinal magnetization showed that the responses are delayed but have the same frequency of the perturbing oscillating field. But unlike the case of the Ising system in periodically varying transverse field (see Sec. III B and Ref. 10), the amount of delay in this case is different for transverse and longitudinal magnetization. We can express the response magnetization $m^\alpha(t)$ as $P^\alpha(\omega(t-\tau_{\text{eff}}^\alpha))$, where P^α denotes the periodic function with the same frequency ω of the perturbing field and τ_{eff}^α denotes the effective delay for the αth component $(\alpha=x,y)$ of the response. We again define the susceptibilities in a "linear" way: Assuming a linear response $m^\alpha(t)\sim m_0^\alpha\exp[i(\omega t-\phi_\alpha)]$, $\phi_\alpha=\omega\tau_{\text{eff}}^\alpha$, for a perturbation $h(t)\sim h_0\exp(-i\omega t)$, the ac susceptibility χ_α is defined as $(m_0^\alpha/h_0)\exp(-i\phi_\alpha)$. This defines then the in-phase and the out-of-phase components of the ac susceptibilities: $\chi_s'=(m_0^z/h_0)\cos(\phi_z)$, $\chi_s''=(m_0^z/h_0)\sin(\phi_z)$, and $\chi_x'=(m_0^x/h_0)\cos(\phi_x)$, and $\chi_x''=(m_0^x/h_0)\sin(\phi_x)$.

The components of the transverse and longitudinal susceptibilities are plotted against the temperature (T) in Fig. 10. Similar variations against Γ (at fixed T) are also shown in Fig. 11. At the dynamic transition point, where the dynamic order parameter Q_z vanishes, the χ_x' and χ_z' give sharp dips and χ_x'' and χ_z'' give sharp peaks. Both χ_x' and χ_z' have another smeared peak at some higher temperature $[T>T_c(\Gamma)]$ (Fig. 10).

3. *Solution in the linearized limits*

It may be noted that the equation of motion for the z component gets completely decoupled in the limits $T^{-1}\to 0$ and $\Gamma\to 0$. We can write from Eq. (11),

$$\tau\frac{dm^x}{dt}=-m^x+\frac{\Gamma}{T}\,,$$
$$\tau\frac{dm^z}{dt}=\left[1-\frac{1}{T}\right]m^z+\frac{h_0\cos(\omega t)}{T} \tag{17a}$$

in the $T^{-1}\to 0$ limit and

$$\tau\frac{dm^x}{dt}=-m^x+\left[\tanh\left[\frac{m^z+h(t)}{T}\right]\right]\frac{\Gamma}{m^z+h(t)}\ ,$$

$$\tau\frac{dm^z}{dt}=-m^z+\tanh\left[\frac{m^z+h(t)}{T}\right] \tag{17b}$$

in the $\Gamma\rightarrow 0$ limit. This suggests that the dynamic transition, etc., for the z component remains qualitatively the same as in the classical mean-field case; the solution in the linearized case is already given there (see Sec. II).

D. Response due to a pulsed transverse field in the absence of longitudinal field

In order to study another interesting dynamic response of such systems, we have studied the response of pulsed transverse field on an Ising system, by solving the dynamical equation of motion (11) for the response magnetization in the mean-field approximation. Specifically, such a case [case (c)] is represented by the Hamiltonian (9), where $h(t)=0$ and the time variation of the transverse field is taken as

$$\Gamma(t)=\Gamma+\delta\Gamma \quad \text{for } t_0\le t\le t_0+\delta t\ ,$$
$$=\Gamma, \quad \text{elsewhere}\ . \tag{18}$$

As mentioned before, such a pulse can be applied to order-disorder ferroelectrics by applying a pressure pulse.[20] Here, the pulse has been applied at the equilibrium. First, we allowed the system to relax to its equilibrium state at any temperature (T) and then we applied the pulse of small amplitude $\delta\Gamma$ and short duration (δt) (compared to the relaxation time of the system) and observed the response of transverse magnetization. Here, the response longitudinal magnetization m^z shows a dip (of height m_p^z and half-width Δ_z measured from the equilibrium value) at the time (i.e., during the active period of the pulse) when the pulse has been applied (see Fig. 12).

The width ratio $R_z(=\Delta_z/\delta t)$ has been measured and we have studied the temperature variation of R_z. Our observation shows that R_z has a very sharp variation, almost diverging [Fig. 13(b)], at the order-disorder transi-

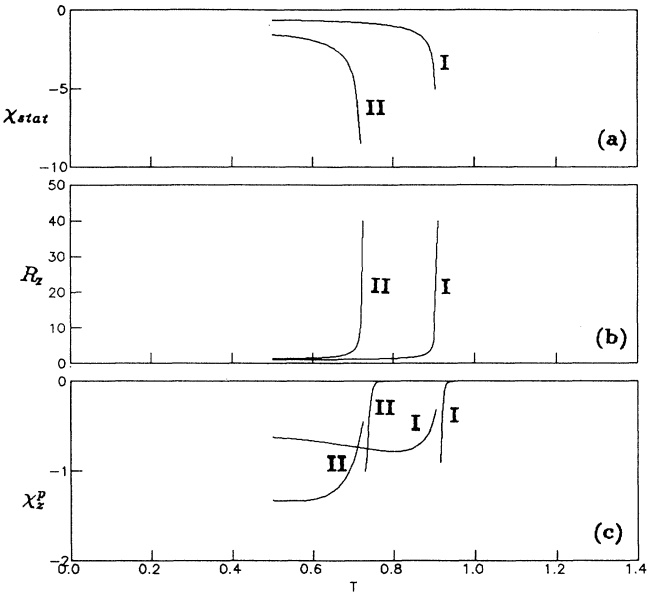

FIG. 13. (a) Variation of the static susceptibility $\chi_{\rm stat}(=dm^z/d\Gamma)$ with respect to T for two different Γ. I: $\Gamma=0.5$ and II: $\Gamma=0.8$. (b) Temperature variation of the width ratio R_z for different Γ for pulsed variation in Γ. I: $\Gamma=0.5$, $\delta\Gamma=0.025$, and $\delta t=50\times dt$ and II: $\Gamma=0.8$, $\delta\Gamma=0.025$, and $\delta t=50\times dt$. (c) Temperature variation of χ_x^p for two different Γ for pulsed variation in Γ. I: $\Gamma=0.5$, $\delta\Gamma=0.025$, and $\delta t=50\times dt$ and II: $\Gamma=0.8$, $\delta\Gamma=0.025$, and $\delta t=50\times dt$.

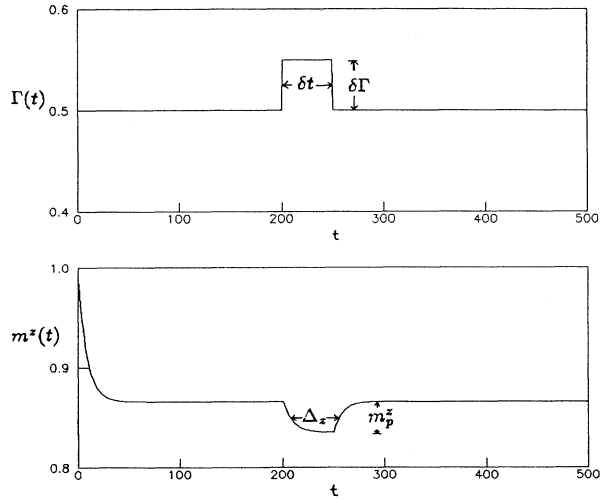

FIG. 12. Time variation of pulsed $\Gamma(t)$ and $m^z(t)$ for a fixed value of the temperature T (=0.2). $\Gamma=0.5$, $\delta\Gamma=0.05$, and $\delta t=50x\ dt$.

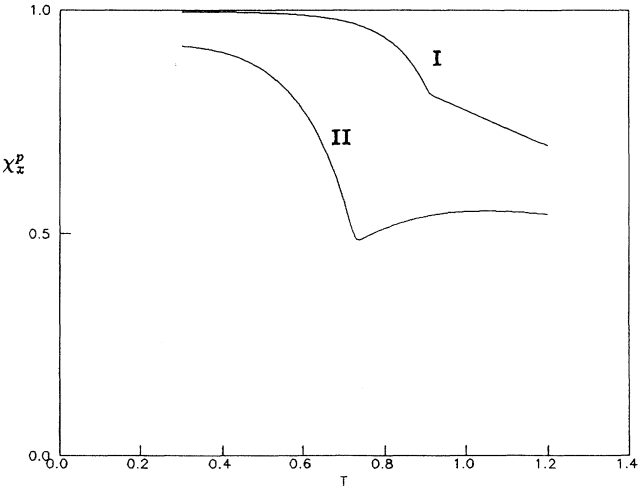

FIG. 14. Temperature variation of χ_x^p for two different values of Γ for pulsed variations in Γ. I: $\Gamma=0.5$ and II: $\Gamma=0.8$. The kinks indicate the transition points for two different values of Γ.

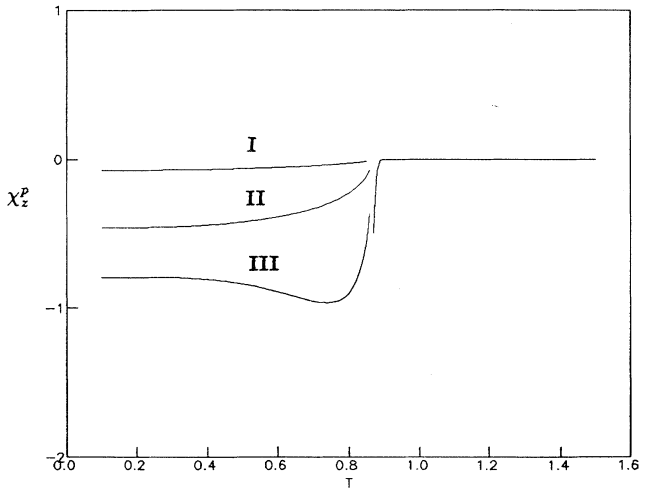

FIG. 15. Temperature variation of χ_z^p for three different values of the pulse width (δt) of the transverse field. I: $\delta t = 2\times dt$, II: $\delta t = 10\times dt$, and III: $\delta t = 50\times dt$. In all cases, $\Gamma = 0.6$ and $\delta\Gamma = 0.05$.

tion temperature [$T_c(\Gamma)$]. We also define and measure the pulse susceptibility $\chi_z^p (= m_p^z/\delta\Gamma)$. We find χ_z^p also to increase (possibly diverge) at the same point [Fig. 13(c)]. It may be noted that χ_z^p becomes identical with the static susceptibility as the pulse width δt increases to infinity (and $\delta\Gamma \to 0$). We also studied the behavior of transverse susceptibility χ_z^p with respect to temperature for the pulsed transverse field. A significant change in the temperature variation in χ_x^p is again observed at the transition point (Fig. 14).

In order to see the effect of the pulse width δt, we have also studied the variation of the pulse susceptibility (χ_z^p) with respect to temperature (at fixed Γ) for the different values of the pulse width (δt) (Fig. 15). For the first case, with $\delta t = 2$, the pulse width being very small compared to relaxation time at all values of T, the response is not very prominent: $\chi_z^p \cong 0$. For a slightly higher value of the pulse width ($\delta t = 10$), we observed the system to respond partially, and as the transition point is approached, the relaxation time increases and the response decreases and finally vanishes. For even higher values of pulse width (e.g., $\delta t = 50$), the response is similar to that of static perturbation [static susceptibility has a sharp dip at $T_c(\Gamma)$]. It is to be noted that as the relaxation time of the system increases much above the pulse width δt, the response again falls to zero.

IV. CONCLUDING REMARKS

We have studied numerically the time variation of the response magnetization $m(t)$ of an Ising system in the presence of a time varying (sinusoidal and pulsed) longitudinal external field $h(t)$, using Glauber-type dynamics with nonconserving order parameter (Sec. II). We have also studied (in Sec. III) the response magnetization [$m^\alpha(t)$, $\alpha = x,y$] for the Ising system in the presence of sinusoidally varying longitudinal field $h(t)$ in the presence of constant transverse field Γ and also in the case of zero external longitudinal field, but the transverse field Γ has a pulsed time variation.

(a) In Sec. II, using both Monte Carlo simulation for ferromagnetic Ising systems (with time-dependent longitudinal field) in one to four dimensions, and solving numerically the mean-field equation of motion, we have investigated the nature of response magnetization $m(t)$ of an Ising system in the presence of a periodically varying external field [$h(t) = h_0 \cos(\omega t)$]. These results are given in Sec. II B. From these studies, we determine the m-h loop or hysteresis loop area $A (= \oint m dh)$ and the dynamic order parameter $Q (= \oint m dt)$ and investigate their variations with the frequency (ω) and amplitude (h_0) of the applied external magnetic field and the temperature (T) of the system.

The variations in A are fitted to a scaling form (1), which is found to be valid over a wide range of parameter (ω, h_0, and large T) values and the best-fit exponents are obtained in all three dimensions ($D = 2,3,4$). The scaling function is Lorentzian (1b) in the MF case and is exponentially decaying, with an initial power law (1a), for the MC cases. These scaling fits for loop area A are discussed in Sec. II C. As mentioned there, we observed the frequency dependence in the above scaling forms to be much more robust than for the other parameters (h_0, T, etc.). Additionally, we observed that the fitting exponent values from the MC results in $D = 4$ do not converge with those obtained from the MF studies.

The dynamic phase boundary (in the h_0-T plane) is found to be frequency dependent and the transition (from $Q \neq 0$ for low T and h_0 to $Q = 0$ for high T and h_0) across the boundary crosses over to a continuous from a discontinuous one at a tricritical point (see Sec. II D). These boundaries are determined in various cases. We find that the response can be generally expressed as $m(t) = P(\omega(t - \tau_{\text{eff}}))$, where P denotes a periodic function with the same frequency (ω) at the perturbing field and $\tau_{\text{eff}}(h_0, \omega, T)$ denotes the effective delay. This equality in the frequency of the response with that of the perturbing field comes from the invariance of the (Glauber dynamics or mean-field) equation of motion for a substitution of $t \to t + 2\pi/\omega$. We established that this effective delay τ_{eff} of the response is the crucial term and it practically determines all of the above observations for A, Q, etc. Investigating the nature of the in-phase (χ') and the out-of-phase (χ'') susceptibility form $\chi = (m_0/h_0)\exp(-i\phi)$, $\phi = \omega\tau_{\text{eff}}$, we find χ'' gives an idea of the loop area and the temperature variation of χ'' at different ω and h_0 gives a prominent peak at the dynamic transition point (see Sec. II E). It also indicates that the dynamic transition is a truly thermodynamic transition. In fact, we also see (Fig. 5) that the dynamic transition ends in the order-disorder transition in the limit $h_0 \to 0$, $\omega \to 0$.

Our study also indicates that, although both A and Q are (dynamic) state functions (of the variables h_0, ω, and T), Q gives a more accurate representation of the dynamic phase than A, which is a multivalued function of the state variables (e.g., $A \to 0$ as $\omega \to 0$ as well as for $\omega \to \infty$; see Fig. 2).

We find that the numerical solution of the (fluctuationless) mean-field equation of motion (3) gives us all the typical features of the hysteretic response and the dynamic transitions observed in the Monte Carlo studies. Moreover, the solution of the linearized mean-field equation of motion in all these cases (see also the Appendix) shows that, although the linear analysis gives all the generic forms for the variation of the quantities like A, Q, and χ (through the effective time lag τ_{eff} or the phase lag $\phi=\omega\tau_{\text{eff}}$), the detailed behavior (and the numerical values of the exponents, etc.) differs significantly from those obtained using linear analysis.

In Sec. II F, we reported the results of the study of the response in the Ising system in the presence of a pulse magnetic field of very short duration (compared to relaxation time). We find a sharp peak in the width ratio and a smeared peak in the pulse susceptibility at the order-disorder transition point of the (unperturbed) system (see Fig. 8 and Sec. II F). This suggests that the study of this pulse susceptibility and the width ratio can give very useful prior indication of the catastrophic transition which is self-organized or self-tuned (e.g., earthquake, fracture, etc.).

(b) In Sec. III, we studied, solving numerically the mean-field equation of motion, the nature of the response magnetization [for the components $m^x(t)$ and $m^z(t)$] of an Ising system in the presence of a periodically varying axial field [$h(t)=h_0\cos(\omega t)$] and a static transverse field (Γ). From these studies (Sec. III C), we studied the dynamic order parameter $Q_z(=\oint m^z dt)$ and investigated its variations with amplitude (h_0) of the applied external axial magnetic field, the temperature (T) of the system, and the externally applied transverse field (Γ). The dynamic phase boundaries (in the h_0-T and h_0-Γ planes) have been drawn and the transition (from $Q_z\neq 0$ for low T, Γ, and h_0 to $Q_z=0$ for high T, Γ, and h_0) across the boundary crosses over to a continuous from a discontinuous one across a tricritical line. It has been observed that the response components (m^z and m^x) are delayed with respect to the oscillating field. We found that the response can be generally expressed as $m^\alpha(t)=P^\alpha(\omega(t-\tau^\alpha_{\text{eff}}))$, where P^α denotes the periodic function with the same frequency ω of the perturbing field and τ^α_{eff} denotes the effective delay for the αth component ($\alpha=x,z$) of the response. Investigating the nature of the in-phase (χ'_α) and the out-of-phase (χ''_α) susceptibility, defined as $\chi'_\alpha=(m^\alpha_0/h_0)\cos(\phi_\alpha)$ and $\chi''_\alpha=(m^\alpha_0/h_0)\sin(\phi_\alpha)$, $\phi_\alpha=\omega\tau^\alpha_{\text{eff}}$ [and m^α_0 is the amplitude of $m^\alpha(t)$], we found that the χ''_α (χ'_α) gives a prominent peak (dip) at the dynamic transition point.

The response [$m^z(t)$] of the Ising system has also been studied for a short-duration pulse (of width δt and height $\delta\Gamma$, over its steady value Γ) of the transverse field (Sec. III A). Induced response (due to pulse) also has a finite width and height. The width ratio (of the half-width of the response with that of the pulse) and the (pulse) susceptibility (the ratio of the height of the induced response with that of the pulse) diverge at the order-disorder transverse point. This study again indicates that the variation of this "pulse width ratio" or the "pulse susceptibility" are very useful dynamical probes to determine the "static" phase diagrams.

All our studies here (for the quantum Ising system) use mean-field equations of motion (11), which arise solely from the contact with the heat bath. However, at extremely low temperature (and for high-frequency measurements), the quantum dynamics should become prominent. For example, in the case of a pulse in transverse field, the change in energy of the system ($\sim\delta\Gamma$) will introduce a "quantum relaxation" time $\Delta t\sim\hbar/\delta\Gamma$, dictated by the uncertainty relation (with $\hbar$ as Planck's constant). In such low-temperature cases (and high-frequency measurements), the above quantum time scale $\Delta t(\sim\hbar/\delta\Gamma)$ will compete with δt, the pulse width. Such considerations are missing in our study and extensions of these studies to such cases would be very useful and necessary.

ACKNOWLEDGMENTS

We are grateful to D. Stauffer and R. B. Stinchcombe for many important suggestions and useful discussions.

APPENDIX: SOLUTION OF THE LINEARIZED MEAN-FIELD EQUATION OF MOTION: LONGITUDINAL FIELD CASE

In the limits $h_0\to 0$ and $T\gg 1$, the equation of motion (3) can be linearized to give

$$\tau\frac{dm}{dt}=-\epsilon m+\frac{h(t)}{T},\quad h(t)=h_0\cos(\omega t),\quad \epsilon=1-1/T\ , \tag{A1}$$

of which the stable solution can be written as

$$m(t)=c_1\cos(\omega t)+c_2\sin(\omega t)=m_0\cos(\omega t-\phi)\ ,\qquad \phi=\omega\tau_{\text{eff}}\ , \tag{A2}$$

where $C_1=h_0\epsilon/T(\epsilon^2+\omega^2\tau_2)^{1/2}$, $c_2=h_0\omega\tau/T(\epsilon^2+\omega^2\tau^2)^{1/2}$, $c_1^2+c_2^2=h_0^2/T^2$, $m_0=h_0/T(\epsilon^2+\omega^2\tau^2)^{1/2}$, and $\phi=\omega\tau_{\text{eff}}=\tan^{-1}(c2/c1)=\sin^{-1}[\omega\tau/\sqrt{(\epsilon^2+\omega^2\tau^2)}]$. The loop area is thus given by

$$A=\oint m dh\sim\frac{h_0^2\omega\tau}{T(\epsilon^2+\omega^2\tau^2)^{1/2}}\sim m_0h_0\cos(\phi)\ , \tag{A3}$$

which will be maximum at $\omega_{\max}=\epsilon/\tau$.

The loop area A can also be expressed in terms of the imaginary part of ac susceptibility in this case: In fact, as defined in Sec. II E, $\chi=(m_0/h_0)\exp(i\phi)$. Using, therefore, the out-of-phase susceptibility $\chi''=(m_0/h_0)\sin(\phi)$, one gets (from A3)

$$A\sim h_0m_0\sin(\phi)\sim h_0^2\chi''\ . \tag{A4}$$

This indicates that the scaling function $g(x)$ in (1), indeed the dissipative (or out-of-phase) part (χ'') of the complex susceptibility (χ), and the variation of $g(x)$ (with T, h_0, and ω) indicate the variation of τ_{eff} and of m_0 [as defined in (4); see also the above results of linear analysis].

*Electronic address: muktish@saha.ernet.in
†Electronic address: bikas@saha.ernet.in

[1]M. Acharyya and B. K. Chakrabarti, Physica A **192**, 471 (1993); **202**, 467 (1994).
[2]G. S. Agarwal and S. R. Shenoy, Phys. Rev. A **23**, 2714 (1981); S. R. Shenoy and G. S. Agarwal, *ibid.* **29**, 1315 (1984).
[3]T. Tome and M. J. de Oliviera, Phys. Rev. A **41**, 4251 (1990).
[4]P. Jung, G. Gray, and R. Ray, Phys. Rev. Lett. **65**, 1873 (1990).
[5]M. C. Mahato and S. R. Shenoy, Physica A **186**, 220 (1992); Phys. Rev. E **40**, 2503 (1994).
[6]M. Rao, H. R. Krishnamurthy, and R. Pandit, J. Phys. Condens. Matter **1**, 9061 (1989); Phys. Rev. B **42**, 856 (1990).
[7]D. Dhar and P. B. Thomas, J. Phys. A **25**, 4967 (1992); P. B. Thomas and D. Dhar, *ibid.* **26**, 3973 (1993).
[8]W. S. Lo and R. A. Pelcovits, Phys. Rev. A **42**, 7471 (1990).
[9]S. Sengupta, Y. J. Marathe, and S. Puri, Phys. Rev. B **45**, 7828 (1990).
[10]M. Acharyya, B. K. Chakrabarti, and R. B. Stinchcombe, J. Phys. A **27**, 1533 (1994).
[11]M. Acharyya and B. K. Chakrabarti, in *Annual Reviews of Computational Physics,* edited by D. Stauffer (World Scientific, Singapore, 1994), Vol. 1, p. 107.
[12]Y.-L. He and G.-C. Wang, Phys. Rev. Lett. **70**, 2336 (1993).
[13]M. Acharyya and B. K. Chakrabarti, J. Magn. Magn. Mater. **136**, L29 (1994).
[14]S. Chikazumi, *Physics of Magnetism* (Wiley, New York, 1964), Chap. 16.
[15]R. B. Flippen, T. R. Askew, and M. S. Osofsky, Physica C **201**, 391 (1992).
[16]L. D. Landau and E. M. Lifshitz, *Electrodynamics of Continuous Media,* Course of Theoretical Physics Vol. 8 (Pergamon, Oxford, 1960), Sec. 45; V. B. Geshkenbeen, V. M. Vinokur, and R. Fehrenbacher, Phys. Rev. B **43**, 3748 (1991).
[17]P. G. de Gennes, Solid State Commun. **1**, 132 (1963); R. B. Stinchcombe, J. Phys. C **6**, 249 (1973).
[18]See, e.g., P. Sen and B. K. Chakrabarti, Int. J. Mod. Phys. B **6**, 2439 (1992).
[19]B. K. Chakrabarti, Rev. Solid State Sci. **2**, 559 (1988); M. Sahimi and S. Arbabi, Phys. Rev. Lett. **68**, 608 (1992); M. Acharyya and B. K. Chakrabarti, J. Phys. (France) I **5**, 153 (1995).
[20]R. Blinc, J. Phys. Chem. Solids **13**, 204 (1960); R. Blinc and M. Ribaric, Phys. Rev. **130**, 1816 (1963); P. S. Peercy, B **12**, 2725 (1975).